Development of a model of phytoplankton blooms in Manukau Harbour

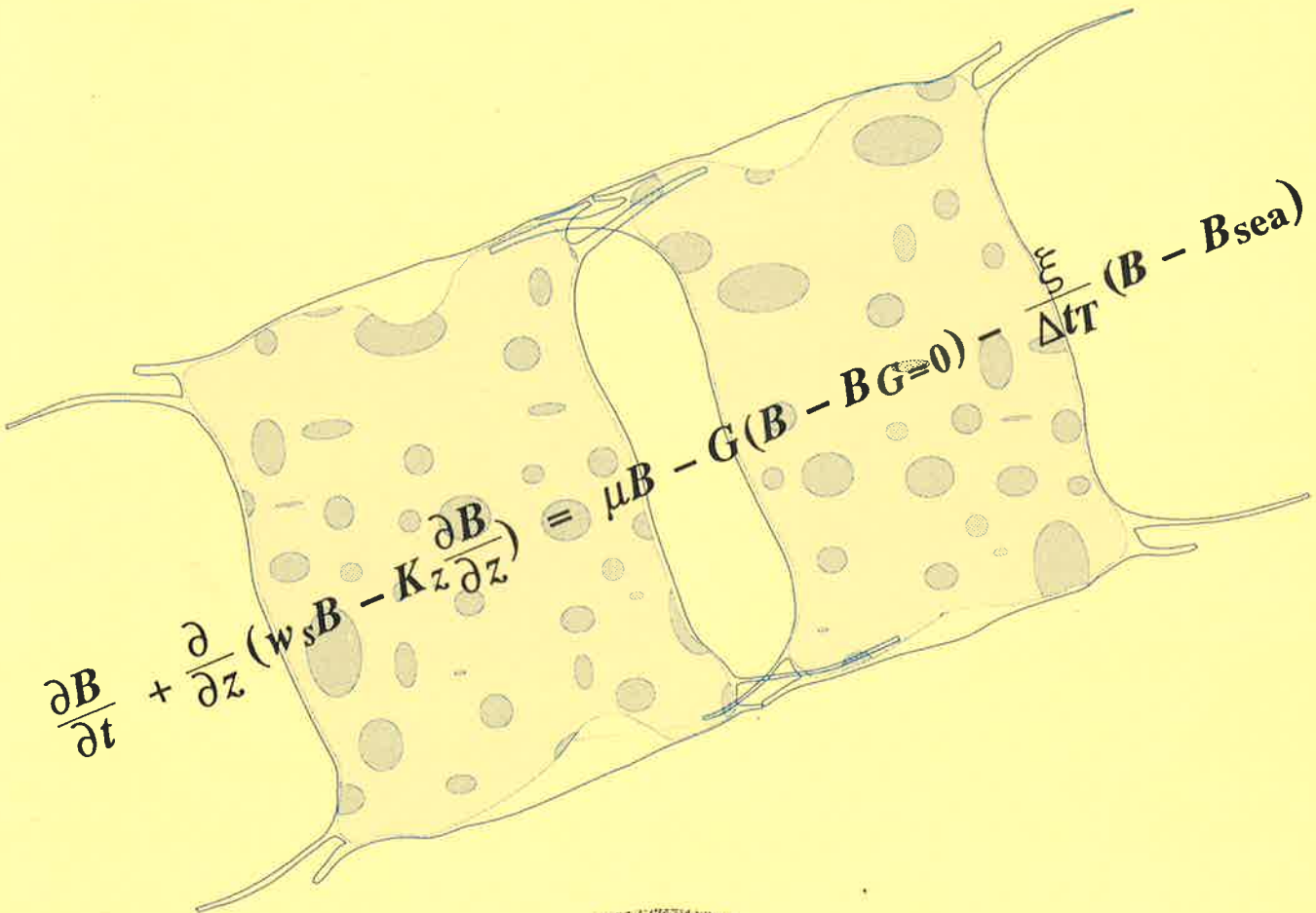

NIWA Ecosystems Publication No. 3
Hamilton, New Zealand
1993

Development of a model of phytoplankton blooms in Manukau Harbour

G. B. McBRIDE, W. N. VANT, J. E. CLOERN*, J. B. LILEY

NIWA Ecosystems
National Institute of Water and Atmospheric Research
Hamilton, New Zealand

*U S Geological Survey, Menlo Park CA, USA

NIWA Ecosystems Publication No. 3
Hamilton, New Zealand
1993

Cataloguing-in-Publication data
McBride, G. B.
Development of a model of phytoplankton blooms in Manukau Harbour / by G. B. McBride, W. N. Vant, J. E. Cloern and J. B. Liley - Hamilton, N. Z. : NIWA Ecosystems, 1993. (NIWA Ecosystems publication; 3)
ISSN 1172–3726
ISBN 0–478–08300–9
I. Vant, W. N.; II. Cloern, J. E.; III. Liley, J. B.; IV. Title; V. Series; VI. National Institute of Water and Atmospheric Research; VII. NIWA Ecosystems.

Cover: Two cells of the large (100–200 μm) diatom *Odontella sinensis* which bloomed in Manukau Harbour in February–March 1992, and the key equation of the computer model BLEST. (Design: R. G. Budd & V. J. Cummings.)

The NIWA Ecosystems publication series supersedes the Water Quality Centre publications.
Available from: NIWA Ecosystems Library, P. O. Box 11-115, Hamilton, New Zealand.

NIWA Ecosystems comprises the former Water Quality Centre and part of the former Taupo Research Laboratory (both ex-DSIR Marine and Freshwater), plus the ex-MAF Technology Aquatic Plants Group and ex-MAF Freshwater Fisheries Group.

ABSTRACT

A mathematical model of phytoplankton blooms in an arm of Manukau Harbour is described. It includes the processes that could be important in promoting and controlling a bloom: cell photosynthesis (driven by incident PAR and its attenuation down the water column); cell respiration; zooplankton grazing; benthic filtering; cell settling; vertical mixing; horizontal mixing. Horizontal advection is accounted for by using a Lagrangian moving frame-of-reference, and horizontal mixing has been incorporated simply, by including a tidal exchange coefficient. In this way the model is restricted to just two independent variables (depth under the reference frame and time), which keeps it relatively simple and allows attention to be focussed on the kinetics of growth and loss. The model has been tested for accuracy with known solutions and is applied to a substantial bloom recorded in the Wairopa Channel in Manukau Harbour in February-March 1992. Broad agreement was obtained between measured and simulated results using plausible values of the model parameters. The critical physical parameters were found to be water depth (via its effect on respiration losses), flushing and water clarity. The critical biological parameters were phytoplankton respiration and community composition, and benthic filtering.

CONTENTS

INTRODUCTION

Phytoplankton populations can increase rapidly in estuaries. For example, spring-time blooms have been recorded consistently in South San Francisco Bay, California (Cloern 1991a). Recently a bloom has been recorded in the Manukau Harbour, Auckland (Vant & Budd 1993). This occurred in the late summer of 1992, in the upper reaches of the Wairopa Channel which extends from Puponga Point to Onehunga (see Fig. 1).

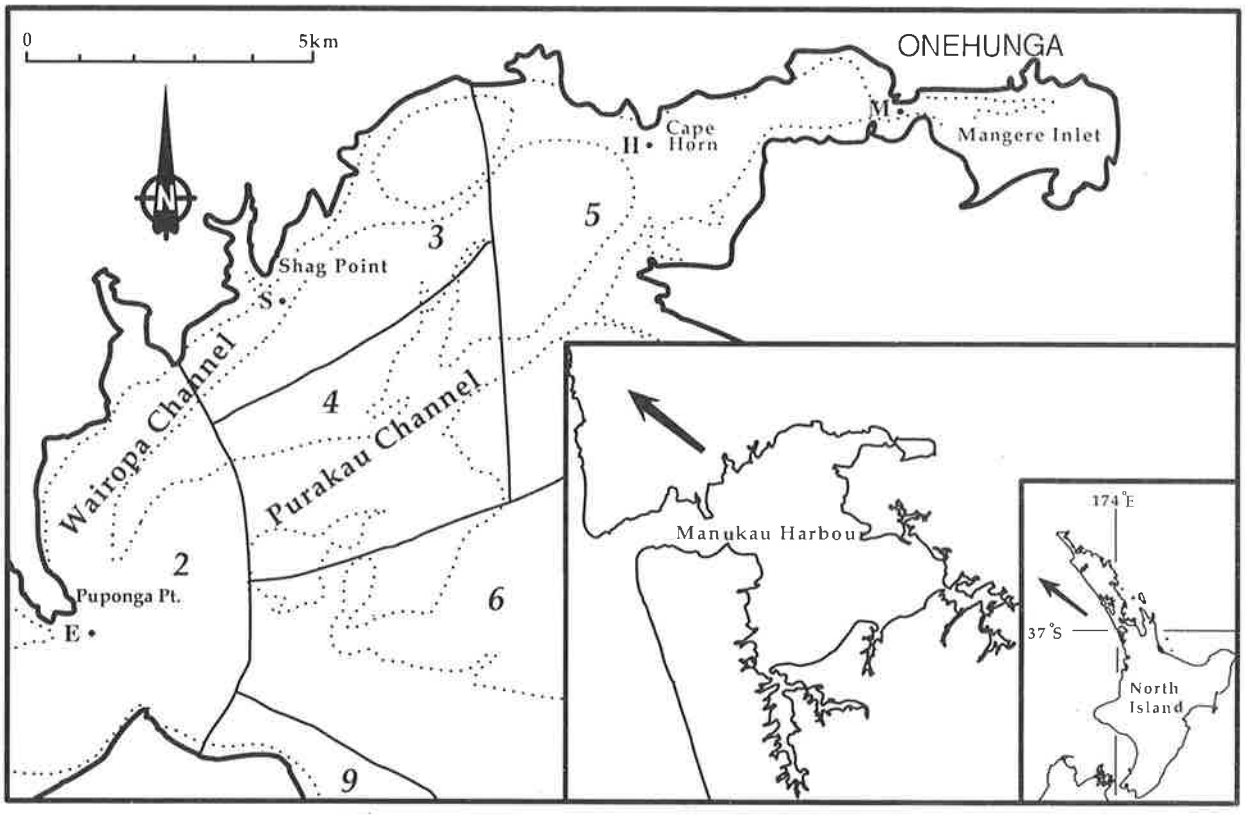

Figure 1 The Wairopa Channel, northern Manukau Harbour. Sampling sites M, H, S, E correspond to sites 1, 2, 3, 4 of Vant (1991). The numbers identify the box-model segments used by Vant & Williams (1992).

The data collected during September 1991–April 1992 from sites M, S and E, are displayed on Fig. 2 (daily tide range, photosynthetically available radiation—PAR, and wind speed are also shown). At Mangere (site M) chlorophyll *a* concentration, a measure of biomass, rose from a background of 5–10 mg m^{-3} to 65 mg m^{-3} during the bloom (similar to the South San Francisco Bay blooms, which typically rise to 45 mg m^{-3} from a background of about 3 mg m^{-3}). These samples were dominated by diatoms (>98% of biovolume), particularly *Odontella sinensis* (51–95% of biovolume). At Shag Point (site S) the chlorophyll *a* concentration during the bloom attained 18.8 mg m^{-3}, and at the harbour entrance (site E) concentrations were always low (< 3 mg m^{-3}).

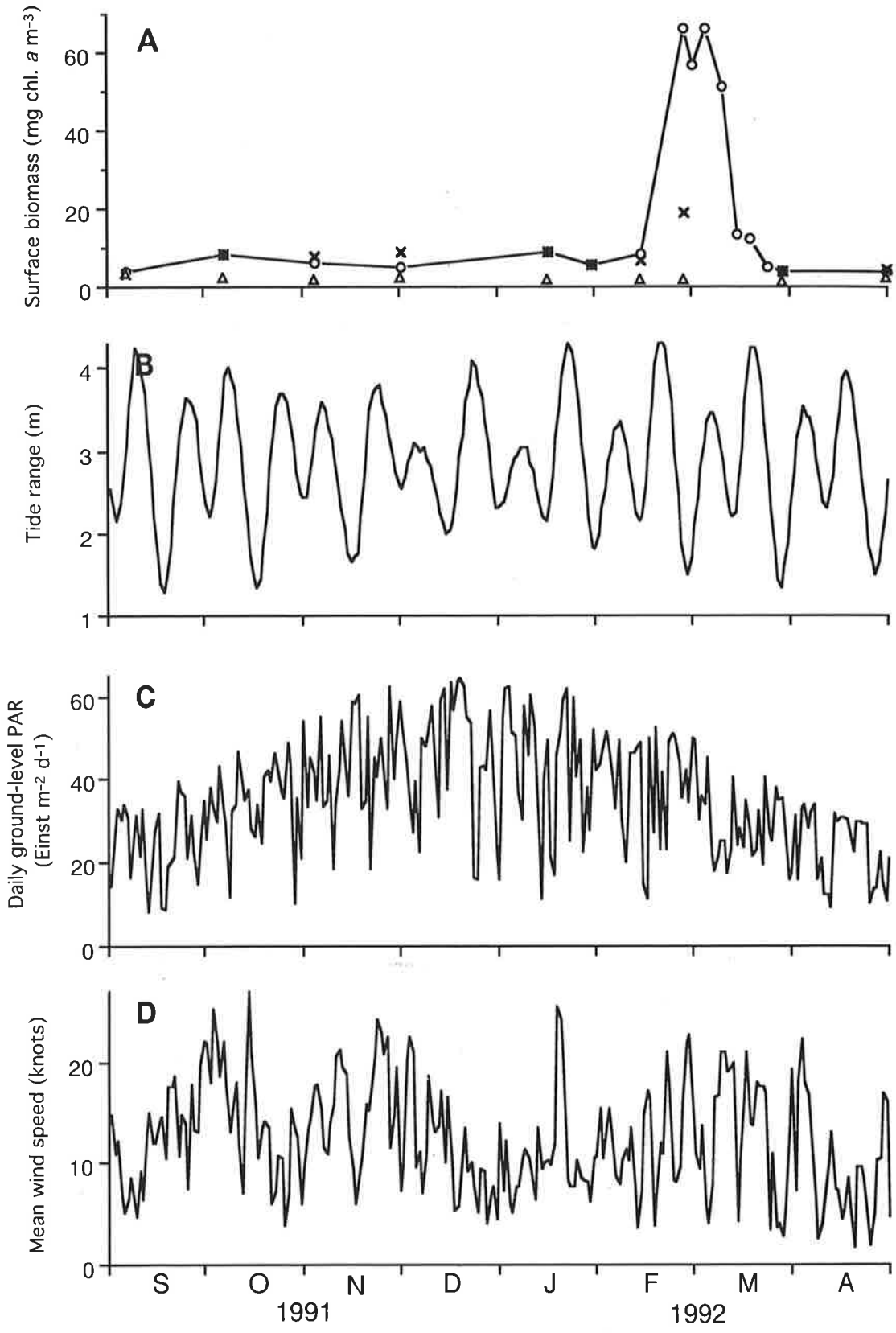

Figure 2 Phytoplankton biomass and environmental conditions in Manukau Harbour, September 1991–April 1992. **A**, Biomass at sites M(o), S(x) and E (Δ), all at high tide (Vant & Budd 1993); **B**, tide range at Onehunga Wharf (Ministry of Transport 1990/1991); and **C**, solar radiation and **D**, wind speed at nearby Auckland Airport (NIWA Climate Database, unpubl. data).

Modelling of this striking phenomenon has the potential to shed light on the predominant causes of phytoplankton growth in the Harbour, and this report presents an initial attempt to do so. The basic approach taken has followed that of Cloern (1991a), which in turn used the framework laid down by Winter *et al.* (1975) for blooms in Puget Sound and by Jamart *et al.* (1977) for blooms in offshore waters. This uses two independent variables: time and depth. The model equations are developed from the principle of conservation of mass, so that information is needed on mixing coefficients, and on the growth and loss rates for phytoplankton. The equations are solved numerically in the program BLEST (BLooms in ESTuaries).

We assume that phytoplankton growth is not limited by nutrient availability during the bloom (although it was observed that inorganic nitrogen levels fell to unusually low values toward the end of the bloom—Vant & Budd 1993—so that silicon levels probably declined as well: Brzezinski 1985). On the basis of past experience, and literature precedent, the major processes to be incorporated are: horizontal advection and mixing; vertical mixing; phytoplankton settling; phytoplankton growth (as affected by temporal and spatial variations in light flux); zooplankton grazing; and benthic filtering by bivalves. Horizontal advection is accounted for by using a Lagrangian moving frame-of-reference, and horizontal mixing has been incorporated simply, by including a tidal exchange coefficient. In this way the model is restricted to just two independent variables (depth under the reference frame and time), which keeps the mixing description relatively simple and allows attention to be focussed on the kinetics of growth and loss. A more complete examination of mixing patterns would require a three-dimensional model, beyond our resources at the present time. In any event, it is desirable to obtain as much explanatory power as possible with the present simpler form. The appropriate values for a number of the parameters are not well-known for Manukau Harbour. We have identified likely values which we use in the simulations described here. We also examine the sensitivity of the model results to changes in the values of the various parameters.

STRUCTURE OF THE MODEL

Units

Mass is always measured in milligrams. The units for photon flux, distance and time depend on the scale of measurement. Our usage differs somewhat from that of Cloern (1991a): i.e.,

- we use μEinst m^{-2} s^{-1} for instantaneous PAR, and Einst m^{-2} d^{-1} for daily PAR (total PAR in 24 hours); Cloern used only the latter (1 Einst m^{-2} d^{-1} = 11.574 μEinst m^{-2} s^{-1}).
- depth is measured in m, but for the vertical mixing coefficient we use cm^2 s^{-1}, as is common; Cloern used m^2 d^{-1} (1 cm^2 s^{-1} = 8.64 m^2 d^{-1}).
- for photosynthesis rate we use mg C (mg chl. *a*)$^{-1}$ h^{-1} (because the data were obtained from short-term incubations: 3–4 h); Cloern used mg C (mg chl. *a*)$^{-1}$ d^{-1} (because his data were from 24 h incubations).

Chlorophyll *a* concentration is the dependent variable, denoted by *B*, and measured in mg chl. *a* m^{-3}.

Time variation

As the purpose of the modelling is to gain information on the progress of chlorophyll *a* concentration (as a surrogate for phytoplankton density), time must always be an independent variable. We denote this by *t*. However, whereas Cloern (1991a) modelled chlorophyll concentrations over the 14 days of a neap-spring cycle, in this exercise we model concentrations over a seasonal time-frame.

Horizontal advection

Modelling of blooms in offshore waters has typically used only one spatial dimension, the depth at a fixed site (Winter *et al.* 1975, Jamart *et al.* 1977, Radach & Moll 1990). This is based on the observation that horizontal gradients of phytoplankton are typically much smaller than those in the vertical, and horizontal currents are usually small. However, in contrast to offshore waters, estuaries and harbours have strong horizontal currents due to the tidal cycle, and these currents will bring waters containing different concentrations of chlorophyll to a site, even if local gradients are relatively small. For this reason using only the depth at a fixed site as the independent variable, ignoring horizontal flows, is not appropriate in estuaries. However if one uses a moving (Lagrangian) reference frame, which moves up or down the harbour as the tide rises and falls, the effect of horizontal flows is much reduced. Such usage takes account of horizontal advection implicitly.

Accordingly, the only spatial dimension used in the model is depth under a moving reference frame. The frame is located at site M (by Onehunga Wharf) at high tide. By low tide it is near site H (Cape Horn) for a neap tide, and is near site S (Shag Point) for a spring tide (based on

the drogue data in Hume 1979). We assume that the frame returns to site M at each high tide. The depth under the frame is denoted by z, the estuary floor being at $z = H$. For South San Francisco Bay Cloern (1991a) used a constant depth (H = 10 m). We also use constant depth, i.e., we assume that the depth under the moving frame remains roughly constant, even though the depth at a fixed site changes through each tidal cycle. This greatly simplifies the input and modelling procedure. Furthermore, we ignore the fact that the harbour has complex bathymetry (i.e., both channels and intertidal areas are present), and simply use the average cross-section depth of the region through which the frame moves (i.e., segments 3, 4 and 5: Fig. 1). From Vant & Williams (1992) the relevant value is H = 3 m. Any photosynthesis—and thus growth of phytoplankton—occurring at greater depths is ignored. This is a reasonable assumption, since the degree of PAR attenuation in this part of the harbour (see later) means that most of the time photosynthesis is confined to the upper 3 m of the water column.

Horizontal mixing

This mixing is caused by local variations of current velocity from the velocity of the reference frame, with the result that some of the water upstream of the frame is exchanged with downstream water. We model the exchange of biomass in this water by:

$$\text{mass exchanged in time } \Delta t = \xi(\bar{B} - B_{sea})\Delta t/\Delta t_T \qquad (1)$$

where:

$\bar{B}$ = average chlorophyll *a* concentration under the frame during time Δt, mg m^{-3};
B_{sea} = average chlorophyll *a* concentration near the harbour entrance;
Δt_T = semidiurnal tidal period (0.53 d);
ξ = tidal exchange coefficient, the proportion of biomass exchanged during Δt_T.

The B_{sea} term is included in eq. 1 to allow some of the biomass downstream of the moving reference frame to augment the upstream biomass. If it were not included, then predicted biomass at the frame could fall to impossibly low levels. We use a value of 2 mg m^{-3}, similar to the average value measured at site E (see Fig. 2A).

Vant & Williams (1992) have applied a box model (using 10 boxes) to the whole Manukau Harbour, using salinity data for calibration. Their exchange coefficient refers to transfer of water over the boundary between adjacent boxes, from one high tide to the next. For the boundary crossing the Wairopa Channel between Cape Horn and Shag Point (see Fig. 1), they found coefficients of 0.05 for each of the boundaries between boxes 5 & 3, and 5 & 4. We use a similar value (0.06: see later).

Vertical mixing

In common with many other studies, we assume that the rate of vertical mixing of phytoplankton biomass can be adequately described by Fick's law. That is, the flux of biomass per unit horizontal area is $-K_z(\partial B/\partial z)$, where $B(z,t)$ is the concentration of biomass and $K_z(t)$ is the vertical mixing coefficient. We assume that K_z is constant both in the vertical and during any given semidiurnal tidal period (Δt_T), but that it may vary between tides. In particular, we may expect that K_z will be higher for spring tides than for neap tides: the greater the tidal range the stronger the current variations.

When identifying appropriate values for K_z it needs to be recognised that even though the model makes explicit use of only one spatial dimension (z), it is in fact two-dimensional (through the use of the moving reference frame). This is important because a mixing coefficient in a one-dimensional model is much greater than in a two-dimensional or three-dimensional model (Yotsukura 1977). (A spatial dimension is removed by averaging currents over that dimension, and so the variability of the current in that direction becomes incorporated into the mixing coefficient.)

In selecting appropriate values we note that literature values are scarce. Cloern (1991a) used K_z = 5–50 m^2 d^{-1} (0.6–5.8 cm^2 s^{-1}) for South San Francisco Bay. The lower value was assumed for neap tides, the latter for spring tides. Lung & O'Connor (1984) applied a tidally-averaged two-dimensional model to salinity distributions in four US estuaries, and obtained vertical diffusion coefficients in the range 0.3–9.0 cm^2 s^{-1}. Of these, the James River (K_z = 2.0–3.0 cm^2 s^{-1}) estuary has the most similar depth to Manukau Harbour. Because of weaker tides, it has a stronger vertical salinity difference however ($\approx$ 2, whereas Vant & Williams 1992 report that the annual average of fortnightly measurements in Manukau Harbour was only 0.2). For no salinity difference, Lung & O'Connor found that K_z = 3.8–9 cm^2 s^{-1}, and these figures may therefore be more appropriate to Manukau Harbour.

Guymer & West (1988) reported on a 1982 study of a reach in the upper Conwy estuary (north Wales) which appears to have a similar tidal range to Manukau Harbour (Guymer & West 1991: Fig. 3). They used a dye tracer and a moving reference frame, but were unable to obtain a flood tide coefficient because of difficulties in obtaining good vertical spatial definition of dye concentration. They found the ebb tide vertical diffusion coefficient to be in the range 6–21 cm^2 s^{-1}. The vertical salinity distribution was not reported (transverse diffusion studies at this site in similar conditions the following year recorded a vertical salinity difference $\approx$ 3, West *et al.* 1986, Guymer & West 1991). West & Cotton 1981 had previously found 14–24 cm^2 s^{-1} for the ebb tide in this reach, and also 32–67 cm^2 s^{-1} for the flood tide.

We infer that for Manukau Harbour K_z in the range 0.6–5.8 $cm^2\ s^{-1}$ (5–50 $m^2\ d^{-1}$), as used by Cloern (1991a) for South San Francisco Bay, is likely to be too low. Salinity stratification can be marked in the Bay, but not in Manukau Harbour. Suppression of vertical mixing by stratification will be therefore be minimal. From the above studies, a typical K_z in these conditions could be taken as 10–20 $cm^2\ s^{-1}$.

Another consequence of low stratification is that the ratio of spring tide K_z to neap tide K_z is likely to be less than that used by Cloern (his ratio = 10). We note that Manukau Harbour tidal streams at spring tide are about double those at neap tide. If K_z is proportional to the product of the depth-mean velocity and depth (Fischer *et al.* 1979: 250), the spring tide K_z should be about three times the neap tide value, at least for non-stratified conditions. Given that vertical salinity differences tend to be greatest at neap tides, we take a maximum ratio of 5.

Following Cloern (1991a) we assume that K_z varies sinusoidally through the neap-spring cycle:

$$K_z = \frac{1}{2}\left[(K_{z,\text{neap}} + K_{z,\text{spring}}) + (K_{z,\text{spring}} - K_{z,\text{neap}}) \cos\left(\pi \frac{t + \Phi}{7.375}\right)\right] \quad (2)$$

as shown on Fig. 3 (Φ is a spring tide phase lag).

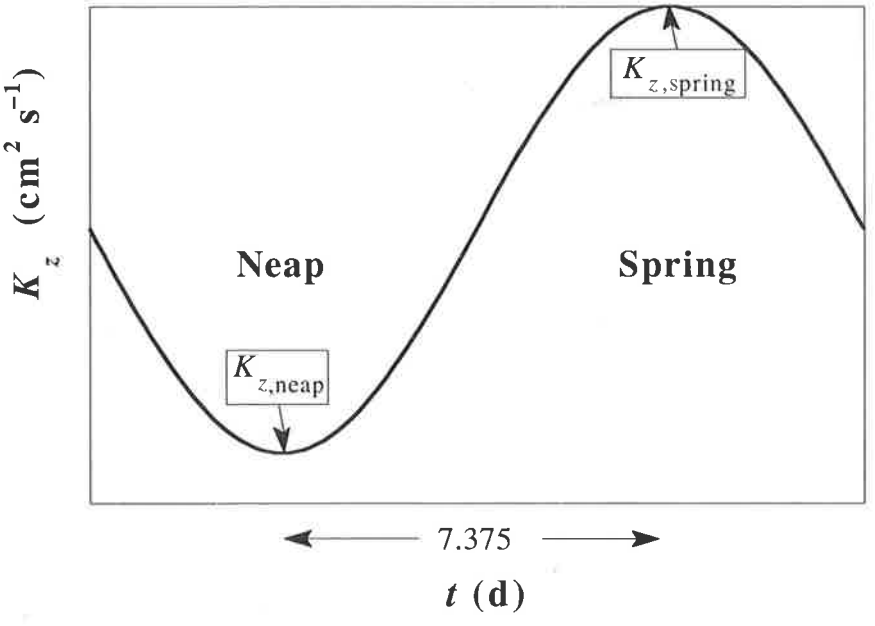

Figure 3 Variation of K_z over the neap-spring tidal cycle.

It is clear from the above that much is yet to be learnt about vertical mixing in estuary flows. Other values of K_z reported in the literature (e.g., Fischer *et al.* 1979, Park & James 1988) show wide variation. This is to some extent associated with the type of estuary studied (many of which are on British coasts with large tidal range), but it would be helpful to obtain more accurate estimates of K_z.

Phytoplankton settling

The settling velocity is denoted by w_s. Cloern used $w_s = 0.5$ m d^{-1}. Smayda (1970) showed how w_s varies with cell size. For example, actively-growing cells of 10–20 μm diameter sink at about 0.5 m d^{-1}, while the rate is an order of magnitude higher for cells of 100 μm. Vant & Budd (1993) observed that cells of this latter size dominated the phytoplankton assemblage during 16 January–24 March 1992, while rather smaller cells were present during the rest of the period shown in Fig. 2. We therefore use $w_s = 5$ m d^{-1} when larger cells were present (16 January–24 March), and $w_s = 0.5$ m d^{-1} at other times.

Phytoplankton growth

To model phytoplankton growth at any time or depth we consider just photosynthesis and respiration. The growth rate of phytoplankton resulting from these two processes is $dB/dt = \mu B$, where B is the concentration of chlorophyll *a* and μ is the specific (i.e., biomass-specific) growth rate (in inverse time units).¶ The gross photosynthesis rate (P) is related to PAR at that time and depth; as P is expressed as mass of carbon per unit mass of chlorophyll *a* (per unit time), a carbon-chlorophyll *a* ratio is required. We follow Cloern (1991a) in assuming that respiration is a constant proportion of the light-saturated photosynthesis rate (P_{max}). The equation for μ at any time or depth can then be written generally as:

$$\mu = \frac{P_{max}}{\theta}[\rho(\iota) - r] \qquad (3)$$

where:

μ = specific instantaneous growth rate, h^{-1};

P_{max} = maximum possible (light-saturated) rate of photosynthesis, mg C (mg chl. *a*)$^{-1}$ h^{-1};

θ = phytoplankton cellular carbon:chlorophyll *a* ratio, mg C (mg chl. *a*)$^{-1}$;

ι = I/I_k is the PAR ratio, dimensionless ($\iota = \iota_0$ just below the water surface);

I = PAR at depth z and time t, μEinst m^{-2} s^{-1};

I_k = saturation onset PAR (the PAR at which the initial slope of the *P-I* curve meets $P = P_{max}$), μEinst m^{-2} s^{-1};

¶ One must be aware of another, different, usage of μ, i.e., growth rate expressed as divisions d^{-1}. Parsons *et al.* (1984) denote this by μ_2 to distinguish it from μ. For constant μ it follows that $\mu = (\ell n 2)\mu_2 = 0.693\mu_2$, and so the doubling time is either $0.693/\mu$ or, equivalently, $1/\mu_2$.

ρ = function relating P to I [i.e., $P = P_{max}\rho(\iota)$], dimensionless ($0 \le \rho \le 1$);
r = phytoplankton respiration rate as a proportion of P_{max}, dimensionless.

During September 1991–April 1992 P_{max} and I_k were measured at monthly intervals at site M (Vant & Budd 1993), and I just above the water (i.e., I_0) was measured continuously (Fig. 2C). These measured values are used here.

The carbon:chlorophyll *a* ratio (θ) was not measured. In general, depending on the assemblage of species present, it can vary widely: Chan (1980) reports θ = 33–35 mg C (mg chl. *a*)$^{-1}$ for diatoms, and θ = 93–120 mg C (mg chl. *a*)$^{-1}$ for dinoflagellates. Vant & Budd (1993) used these values, together with the observed relative abundance of these two groups (no others were important), to calculate assemblage-average values of θ. Dinoflagellates dominated during September–December 1991, diatoms dominated during February–March 1992, while both groups were abundant at other times. The corresponding mean values of θ were 77, 35 and 50 mg C (mg chl. *a*)$^{-1}$. Here we use the values of θ calculated by Vant & Budd (1993) for each of the 16 occasions during September 1991–April 1992 that microscopic analyses of the phytoplankton assemblage were made, and obtain values for the remainder of the period by interpolation.

Likewise, the respiration rate as a proportion of maximal photosynthesis (r) has not been measured. Reviewing many previous studies, Geider & Osborne (1989) observed that values of r range from < 0.1 to about 0.5. Furthermore, they showed how r varied with algal class: dinoflagellates having rather higher values (mean 0.35) than diatoms (~ 0.1), for example. Here we assumed values of 0.35 and 0.10 for dinoflagellates and diatoms respectively, and calculated assemblage-average values as we did for θ. During September–December 1991 and February–March 1992 mean values of r were 0.25 and 0.11 respectively, with a mean value of 0.15 at other times.

Values of μ can be calculated for the data we used, and also for the data used by Cloern (1991a). This requires that one must specify the form of the *P-I* light function (i.e., specify the form of ρ versus ι). Cloern used the equation of Jassby & Platt (1976), i.e., $\rho(\iota) = \tanh(\iota)$, as we do also. It should be noted that by calculating the daily average specific growth rate ($\bar{\mu}$), we can determine the phytoplankton doubling time. The procedures for doing so are given in Appendix 1.

Variation of PAR with time through the tidal cycle

Incident PAR varies through each day. Previous data for the daily distribution of incident PAR in the Auckland area (McBride *et al.* 1991) suggest that a slightly skinny half-sinusoid is the appropriate form to use, at least for cloudless summer days. We adopted:

$$I_0(t) = \begin{cases} I_{0,\max}\sin^n(\pi\tau) & \text{for } 0 \le \tau \le 1 \\ 0 & \text{else} \end{cases} \quad (4)$$

where:

$I_{0,\max}$ = PAR at solar noon just under the water surface (≈ 2200 μEinst m^{-2} s^{-1} for a cloudless Auckland mid-summer day); values were calculated from incident PAR, assuming reflective losses of 5%;

n = PAR distribution shape index, dimensionless (n = 1 gives a regular sinusoid; the shape becomes increasingly skinny as n increases above unity);

τ = $(t-t_{\text{sunrise}})/\Delta t_p$, the fraction of photoperiod, dimensionless;

Δt_p = $t_{\text{sunset}} - t_{\text{sunrise}}$, the photoperiod length, d.

The value of n must be selected carefully. Parsons *et al.* 1984 (using results from Japanese studies in the 1960s) suggested choosing n = 3 for fine days. Denoting the daily insolation by Q, we can show, by simple integration, that $Q_{n=3} = 4I_{0,\max}\Delta t_p/(3\pi)$, whereas for a regular sinusoid (n = 1) it is $Q_{n=1} = 2I_{0,\max}\Delta t_p/\pi$. The assumed shape of the daily PAR variation is therefore important—for the same maximum daily PAR ($I_{0,\max}$) choosing n = 1 gives 50% more daily insolation than for n = 3 (see Fig. 4). However data collected near Auckland, in February 1991, suggest that n = 3 is likely to seriously underestimate daily insolation, and that n = 1.3 is optimal (Fig. 5). In this case $Q_{n=1.3} \approx 0.59I_{0,\max}\Delta t_p$ (obtained by integrating eq. 4 over the photoperiod, for n = 1.3). It may be noted that Platt *et al.* (1990)—considering integer values only for n—found that n = 3 was never appropriate, and that n = 2 only became appropriate for long days at high latitudes.

Variation of PAR with depth

Having obtained the daily variation of incident PAR, $I_0(t)$, we must account for its attenuation down the water column under the reference frame. Cloern (1991a) assumed an exponential depth-wise attenuation (i.e., the Beer-Lambert law, which holds for monochromatic light, was assumed to hold for PAR also). While not stated in his paper, the attenuation coefficient was inflated by the degree of self-shading by the phytoplankton. The equation is:

$$I(z,t) = I_0(t)e^{-\zeta} \quad \text{where} \quad \zeta = \int_0^z K_d(s)\,ds \quad (5)$$

and:

ζ = optical depth, dimensionless;

K_d = $k_x + k_cB$ = vertical PAR attenuation coefficient, m^{-1};

k_x = vertical PAR attenuation for water and its non-algal constituents, m^{-1};

k_c = self-shading coefficient for phytoplankton, m^2 (mg chl. a)$^{-1}$.

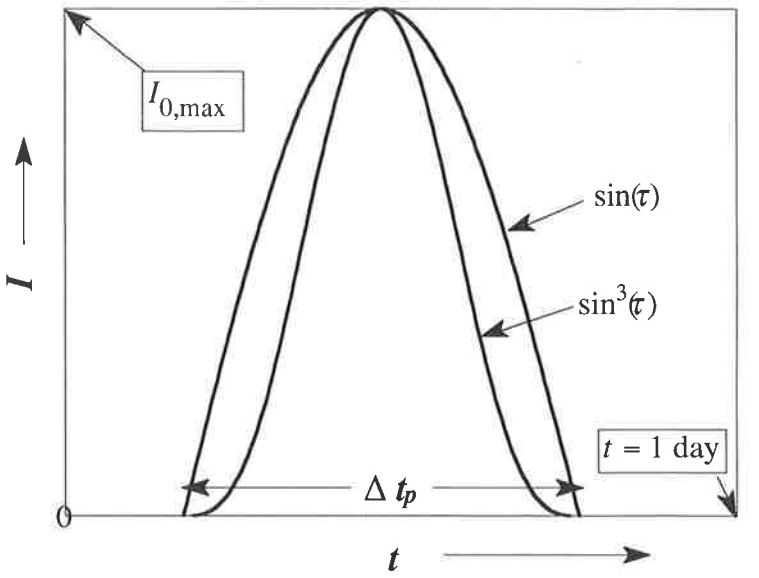

Figure 4 Contrast of daily insolation (the area under the *I*-*t* curve) for n =1 vs. n = 3.

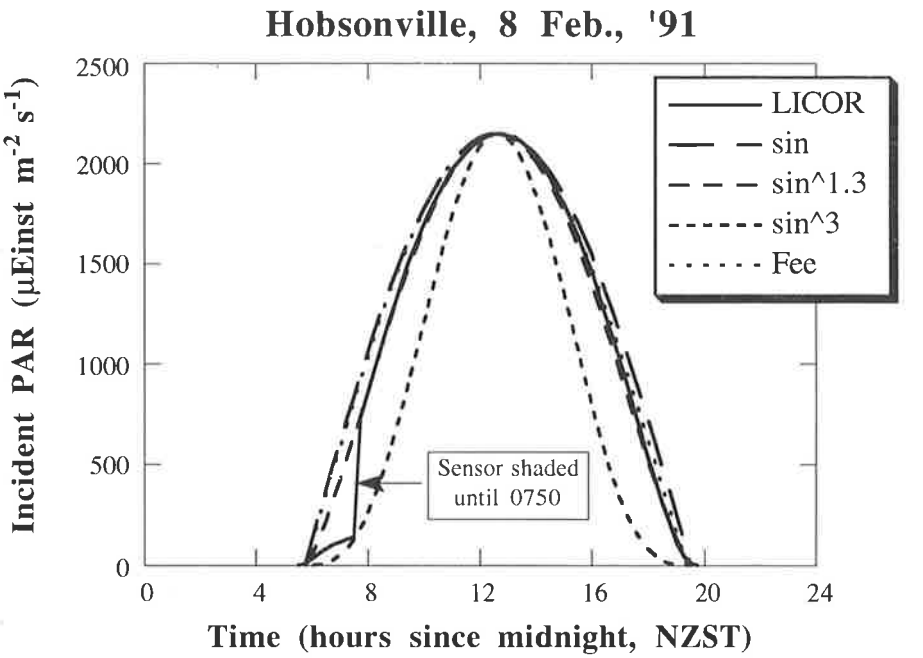

Figure 5 Fitting incident PAR (I_0) data with literature formulae. "LICOR" = data collected (15 minute intervals) on a cloudless day beside SH16, near Hobsonville, using a LICOR 190SB Quantum Sensor. "sin" = fit using a regular sinusoid between sunrise and sunset (5.75 h and 19.5 h, Ministry of Transport 1990), and the inspected PAR maximum. "sin^1.3", "sin^3" = fits using power sinusoids. "Fee" = calculations made from the procedure described by Fee (1990:7), as elaborated in Appendix 2.

Cloern (1991a) used k_x = 1.3 m^{-1}. His paper omits any discussion of self-shading, but his program used the value based on Bannister (1974), k_c = 0.016 m^2 (mg chl. a)$^{-1}$. He multiplied k_c by B at 1 m depth, approximately the midpoint of the euphotic zone, through which phytoplankton biomass is reasonably evenly-distributed. In BLEST we multiply k_c by the value of B in each control volume.

Much of the time observed PAR attenuation and phytoplankton biomass in the northern Manukau Harbour are consistent with k_c = 0.02 m^2 (mg chl. a)$^{-1}$ (Vant & Budd 1993). However, we can expect k_c to decrease with increasing cell size (Kirk 1975). For a large cylindrical diatom like *O. sinensis* we could expect k_c = 0.004 m^2 (mg chl. a)$^{-1}$, with high scattering in the waterbody causing the effective value to be at least twice this (Kirk 1976). We therefore use k_c = 0.01 m^2 (mg chl. a)$^{-1}$ during 16 January–24 March 1992 when large diatoms were observed to dominate the assemblage (see earlier), and k_c = 0.02 m^2 (mg chl. a)$^{-1}$ at other times.

Variation of non-algal attenuation

Vant (1991) showed how mid-tide values of K_d at site M during 1987–88 could be predicted knowing daily tidal range and wind speed. Using data in Vant (1991) and Vant & Smith (1991) we repeated that analysis for high tide values of k_x (= $K_d - k_c B$). The resulting regression equation:

$$k_x = 0.40R + 1.62\left[\frac{U_d^2 + U_{d-1}^2 + 0.1(U_d^3 + U_{d-1}^3)}{2000}\right] - 0.08 \qquad (6)$$

where R is the mean daily tide range (m), U_d is the mean daily wind speed (knots) and U_{d-1} is the value on the preceding day, accounted for 76% of the observed variability in k_x during 1987–88. Values of k_x calculated using eq. 6 and the relevant results in Fig. 2 agreed well with those measured on 11 occasions at site M during September 1991–April 1992 (Vant & Budd 1993). Eq. 6 was therefore used to calculate daily k_x during September 1991–April 1992.

For a fixed reference frame one can expect there to be variation *within* tides also: k_x would be maximal at low tide, because the site will have received turbid inter-tidal water, and will contain clearer water at high tide. However, water under a moving reference frame can be expected to have maximum k_x at mid tide, when currents are strongest. We have made the rough assumption that this within-tide variation can be ignored: k_x is therefore a tidal-average. Indeed, averaged fortnightly data for the 1987/88 year show only a 4% difference between K_d (and hence k_x) at high tide at Onehunga (site M, see Fig. 1) and the mean of low tide K_d at sites H & S (recall that the tidal excursion extends from site M to site H at neap tide, and to site S at spring tide).

Zooplankton grazing

The biomass-specific zooplankton grazing rate is denoted by G (d^{-1}). Cloern *et al.* (1985) calculated G for San Francisco Bay based on the observed abundance of the zooplankton present, and an estimate of the daily feeding rates of the various species. Very little is known about zooplankton in Manukau Harbour. However, assuming community composition and abundance are similar to those reported for the nearby Waitemata Harbour (see Figs 10–41 in Jillett 1971), and that the carbon content of particular species is the same as that of animals of the same genus in San Francisco Bay, we obtain:

$$G = \begin{cases} -\ell n\left(\dfrac{B\theta - F}{B\theta}\right) & \text{for } B > B_{G=0} \\ 0 & \text{else} \end{cases} \qquad (7)$$

where for summer conditions the upper bound to F, the total daily zooplankton ingestion rate (mg C m^{-3} d^{-1}), is given by (after Cloern *et al.* 1985):

$$F = 7.6(1 - e^{-0.01(B - B_{G=0})\theta}) \qquad (8)$$

We used values of G calculated this way in our simulations. Note that eqs 7 and 8 identify a threshold biomass below which grazing does not occur (symbol $B_{G=0}$), as is commonly found in the sea for example (Parsons *et al.* 1984: 133). We have assumed $B_{G=0}$ = 1 mg m^{-3}.

Benthic filtering

Benthic filtering may control phytoplankton biomass in estuaries. This has been demonstrated for clams and mussels in South San Francisco Bay (Cloern 1982, Officer *et al.* 1982), and for cockles and mussels in the Oosterschelde, The Netherlands (Herman & Scholten 1990). There are similar indications for mussels in the Wadden Sea (Asmus & Asmus 1991).

The benthic filtering rate can be quantified by α, defined as the volume of water filtered by benthic bivalves per unit time per unit bed area, measured in the units m^3 m^{-2} d^{-1} (i.e., m d^{-1}). The most important intertidal benthic bivalves in Manukau Harbour are *Austrovenus stutchburyi*, *Mactra ovata* and *Crassostrea gigas* (much less being known about the animals present in the channels). Median sizes of individuals of these species occurring in northern Manukau Harbour are about 26, 40 and 75 mm respectively (Bioresearches 1987, and Auckland Regional Council, unpubl. data). Using flesh dry weights per animal of 0.13 g (see Vant & Smith 1991), 0.42 g and 1 g (e.g., Deslou-Paoli *et al.* 1992), and the relationships in Møhlenberg & Riisgård (1979), we can calculate filtering rates per individual under laboratory conditions of about 2, 3 and 6 l h^{-1} respectively.

For segments 3, 4 and 5 *Austrovenus* are present across the intertidal zone at average densities of about 4, 3 and 45 m^{-2} respectively; while the values for *Mactra* are about 3, 3 and 7 m^{-2} (R. D. Pridmore, and Auckland Regional Council, unpubl. data). *Crassostrea* are present at an average density of 241 m^{-2} (Bioresearches 1987); the area of available habitat can be calculated as the length of rocky coastline (6.1 km in segment 3, and 8.1 km in segment 5) times the width of the zone occupied, assumed to be 10–100 m. If we assume *Crassostrea* are filtering half of the time (i.e., at tide heights above mean sea level), and the *Austrovenus* and *Mactra* present in an area equivalent to the part of the intertidal zone submerged at mean sea level are always filtering, then the volume of harbour water filtered by each of these species is as shown in Table 1.

Table 1 Volume of harbour water filtered by intertidal bivalves

		Segment 3	Segment 4	Segment 5
Area of intertidal below MSL (10^6 m^2)		5.49	8.79	16.11
Austrovenus	- density (m^{-2})	4	3	45
	- number filtering (10^6)	22	26	725
	- volume filtered (10^6 m^3 d^{-1})	1.0	1.3	34.8
Mactra	- density (m^{-2})	3	3	7
	- number filtering (10^6)	16	26	113
	- volume filtered (10^6 m^3 d^{-1})	1.2	1.9	8.1
Crassostrea	- density (m^{-2})	241	-	241
	- number filtering (10^6)	14.7–147	-	19.5–195
	- volume filtered (10^6 m^3 d^{-1})	1.1–10.6	-	1.4–14.1

If we use the value at the midpoint of the range for the *Crassostrea*, the total volume filtered is:

$$[37.1\ (\textit{Austrovenus}) + 11.2\ (\textit{Mactra}) + 13.6\ (\textit{Crassostrea})] \times 10^6\ m^3\ d^{-1}$$
$$= 61.9 \times 10^6\ m^3\ d^{-1}$$

Note that most (82%) of this occurs in segment 5.

To calculate α we need to divide this volume per day by the total area at (mean) high water (i.e., intertidal plus channels). For segments 3, 4 and 5 the value is 70.6×10^6 m^2, giving a value for α of 0.88 m d^{-1}.

Channels occupy 20.9×10^6 m^2 of these segments, and if bivalves there filtered at only one fifth the specific rate of those in the sub-MSL intertidal (= $[61.9 \times 10^6\ m^3\ d^{-1}]/[30.4 \times 10^6\ m^2]$ = 2.1 m d^{-1}), then they would filter a further 8.8×10^6 m^3 d^{-1} (= 0.2 x 2.1 m d^{-1} x 20.9×10^6 m^2), giving a total of 70.7×10^6 m^3 d^{-1}, so that α = 1 m d^{-1}, the value we use here.

Differential form of the equations

All the above defines an initial and boundary value problem which can be written concisely for the unknown $B(z,t)$ as:

$$\frac{\partial B}{\partial t} + \frac{\partial}{\partial z}\left(w_s B - K_z \frac{\partial B}{\partial z}\right) = \mu B - G(B - B_{G=0}) - \frac{\xi}{\Delta t_T}(B - B_{\text{sea}}) \tag{9}$$

with the initial condition (at $t = 0$, for any z):

$$B(z,0) = B_i \tag{9a}$$

where B_i must be prescribed. The boundary conditions (at $z = 0$ and H, for any t) are:

$$\left(w_s B - K_z \frac{\partial B}{\partial z}\right)_{z=0} = 0 \tag{9b}$$

$$\left(w_s B - K_z \frac{\partial B}{\partial z}\right)_{z=H} = \alpha B_{z=H} \tag{9c}$$

where α (m d^{-1}) must be prescribed. It is assumed that the benthic bivalves remove all biomass from the water they filter.

Note that Cloern (1991a) has the third-to-last term of eq. 9 as $(\mu - r)B$, but this was a typographical error.

Method of solution

Although the problem posed by eqs. 9 is linear, analytical solutions have not been found (because of the dependence of coefficients K_z and μ on t). Accordingly, approximate numerical solutions must be obtained. This involves solving a discrete form of eqs 9 on a depth-time grid. We have used the control-volume approach to derive the scheme of equations, as described in Appendix 3. It has been implemented in a PC FORTRAN code, using double-precision arithmetic to minimise rounding errors. The code is written in user-friendly form, with these features:

- input and output variables are always displayed with their units;
- multiple runs can be performed during a single session;
- current input data can be checked at any time, and overwritten for a new run;
- results of a run can be displayed in digit form on a single screen;
- full results, including a listing of all input data and units, are posted to an output file.

Accuracy of solutions

The BLEST code has been run with test cases for which the analytical solution is known, as explained in Appendix 4. Excellent accuracy was obtained, giving good confidence in results obtained for more complex cases. In view of the results obtained, the time-weight (see eq. A3.3) was set at $\omega = 0.5$. Note that using the control-volume approach guarantees that the code is fully mass-conservative. Other schemes (as may be developed from the finite difference approach) may not be, see Appendix 5.

APPLICATION TO MANUKAU HARBOUR

The challenge for this model is to see whether it can mimic the bloom as depicted on Fig. 2A. If it can, using plausible values of the parameters, then it may shed light on conditions for which blooms may recur in the future, and help to guide investigations into the key processes.

To examine this we used a number of plausible values of the model's coefficients, as outlined previously. These all used the Jassby-Platt equation with time-varying PAR, Δt = 1 hour, and $\Delta z = H/100$ m. Fig. 6 shows the simulated values of surface chlorophyll *a* at site M at high water during September 1991–April 1992 (with later starting dates in the period September–January giving virtually identical results). The measured values are also shown. Apart from a substantial discrepancy in the middle of February, there is broad agreement between measured and simulated values. In particular (i) values are generally low until January, (ii) they increase to about 60 mg m^{-3} at the end of February, and (iii) fall around the middle of March and remain low through to the end of the period. Table 2 lists the parameters used in this "best fit" simulation.

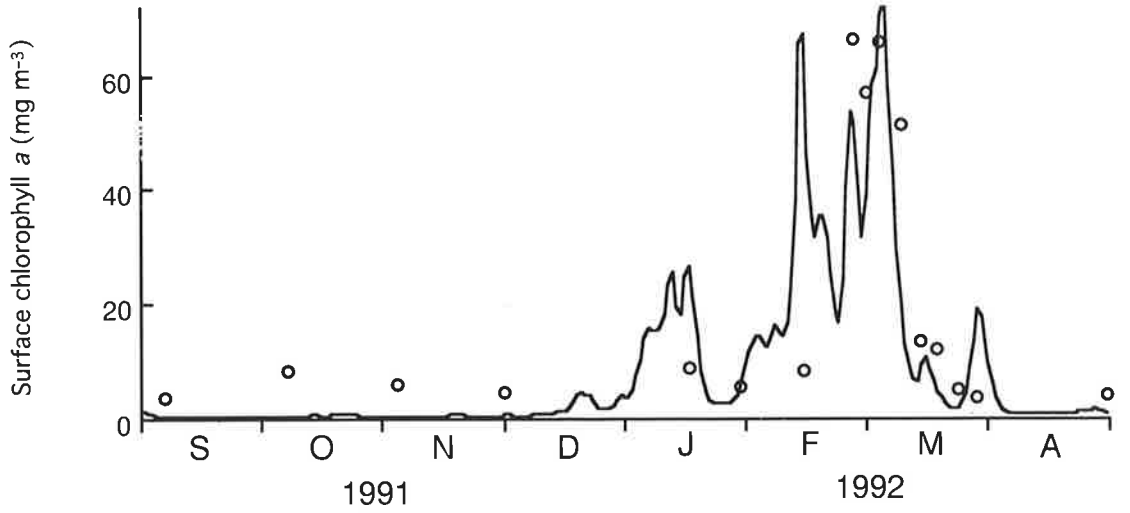

Figure 6 Measured (o) and simulated (line) surface biomass at high tide, site M. Parameters for the simulation are shown in Table 2.

Mean daily growth rate averaged through the water column (eq. A1.7, see Appendix 1) peaked at 0.92 d^{-1} (i.e., a doubling time of 0.75 d) on 12 February. During February–March 1992, when growth was appreciable, the mean rate was 0.39 d^{-1} (corresponding to a doubling time of about 2 d). Growth rates during this period were strongly correlated with the average level of PAR in the water column ($= I_0[1-\exp\{-\zeta_{z=H}\}]/\zeta_{z=H}$) (correlation coefficient = 0.90, n = 60), reflecting the dominant role of underwater PAR in controlling phytoplankton growth (as expected from eq. 3). The important sinks for phytoplankton carbon at this time were

respiration and benthic filtering, which accounted for an average of 52% and 37% of the carbon removed from the system respectively; flushing losses were less important (10%), and zooplankton grazing was only a minor sink (1%).

Table 2 Parameter values used for the "best fit" simulation (see Fig. 6).

B_i	2 mg chl. *a* m^{-3}
B_{sea}	2 mg chl. *a* m^{-3}
G	eqs 7 and 8, with $B_{G=0}$ = 1 mg chl. *a* m^{-3}
r	0.10–0.35, depending on the observed composition of the phytoplankton assemblage
θ	34–106 mg C (mg chl. *a*)$^{-1}$, depending on the observed composition of the phytoplankton assemblage
α	1 m d^{-1}, see Table 1 and following text
k_c	0.01–0.02 m^2 (mg chl. *a*)$^{-1}$, depending on cell size of observed assemblage
w_s	0.5–5 m d^{-1}, depending on cell size of observed assemblage
k_X	eq. 6
P_{max}, I_k	measured values (Vant & Budd 1993)
ξ	0.06
$K_{z,neap}$	10 cm^2 s^{-1}
$K_{z,spring}$	30 cm^2 s^{-1}
H	3 m

The effects of changing the values of certain of the parameters are illustrated in Figs 7–10. In many cases simulated values of surface chlorophyll *a* were low (< 3 mg m^{-3}) during September-December 1991, so only the results from January 1992 are shown in Figs 7 and 9.

Figs 7 and 8 show the effects of changing the important physical parameters. The simulations were sensitive to water depth (Fig. 7A). At H > 5 m levels of biomass were low (< 5 mg m^{-3}). This was due to increased respiration losses in the aphotic zone. As photosynthesis is usually restricted to the upper 3 m, any additional depth imposes an increased respiratory sink for the phytoplankton community.

Large changes in the tidal exchange term produced marked changes in simulated biomass (Fig. 7B). For ξ > 0.3 blooms did not occur (biomass < 10 mg m^{-3}). Lower levels of biomass were also produced by low values of K_z (Fig. 7C), presumably because weaker circulation of cells through the euphotic zone reduces overall photosynthesis. But the simulations were reasonably insensitive to substantial (e.g., 5-fold) increases in K_z.

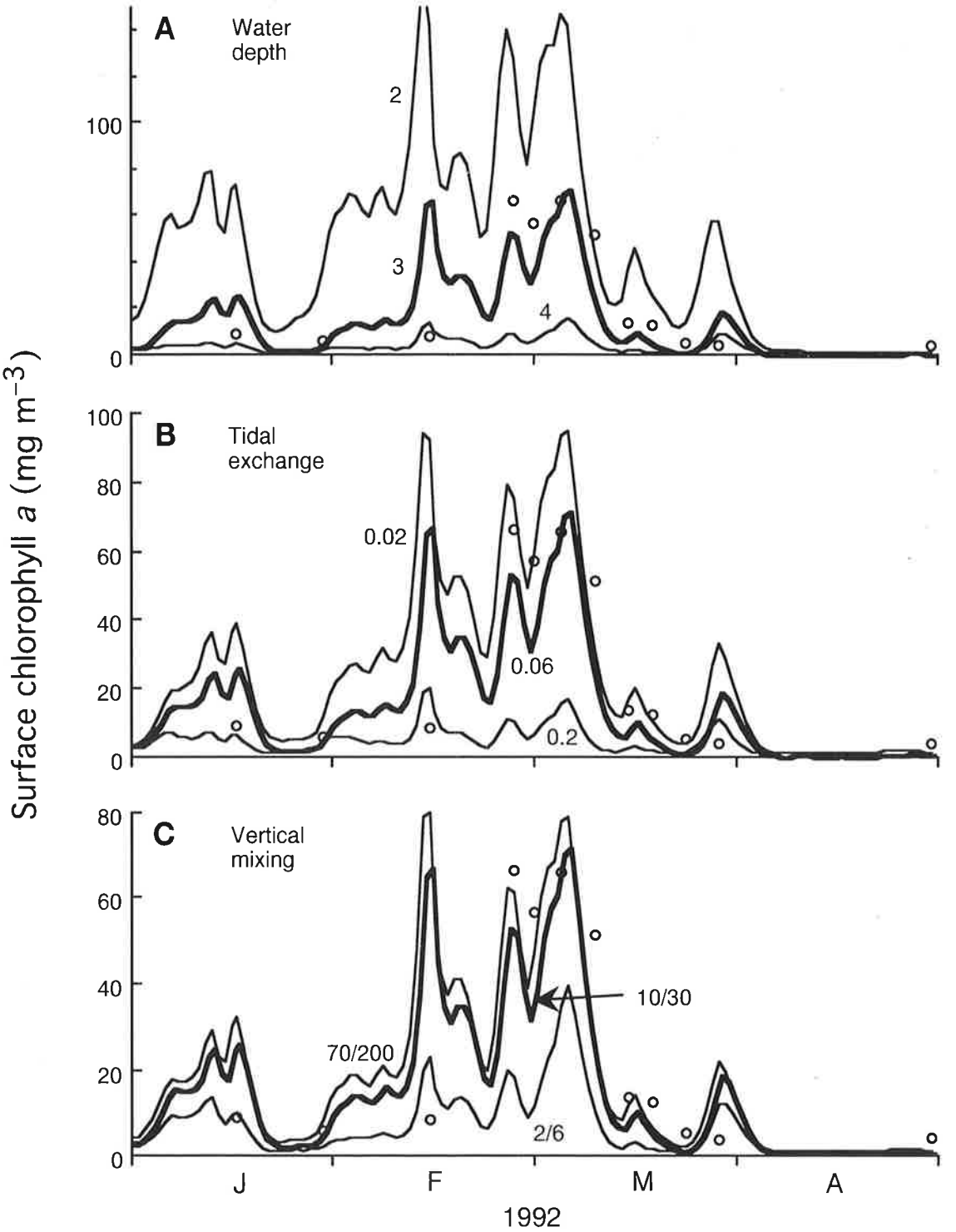

Figure 7 Effects on simulated biomass of varying certain physical parameters as follows: **A**, water depth (H); **B**, tidal exchange (ξ); and **C**, vertical mixing coefficients ($K_{z,\text{neap}}/K_{z,\text{spring}}$). Parameters for the thick lines are given in Table 2, with alternative values noted on each of the other lines.

For September 1991–April 1992 the mean value of calculated k_x was 1.85 m^{-1}. Fig. 8 shows the effect of lower values of k_x (i.e., clearer water) on growth: blooms occurred earlier and reached higher levels (although the very high levels shown here are probably not realistic, since the vigorous growth required could be expected to deplete nutrient levels and thus restrict growth). Similarly, if the contribution of wind to calculated k_x during March-April was ignored, the bloom continued for 3–4 weeks more (results not shown).

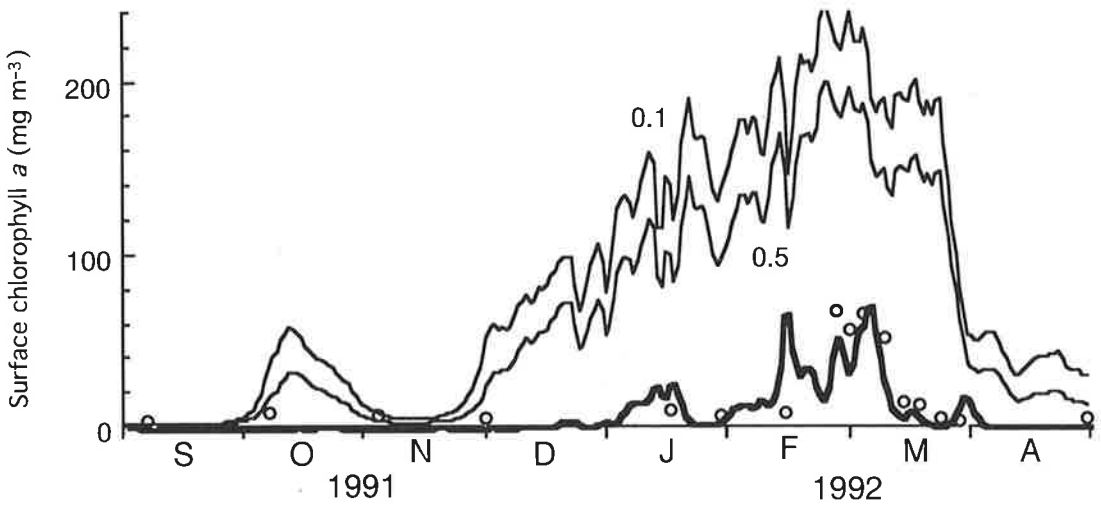

Figure 8 Effect of varying non-algal PAR attenuation (k_x). The thick line shows results obtained using the calculated (eq. 6) values of k_x (mean = 1.85 m^{-1}), while the other lines are for k_x held constant at 0.1 m^{-1} (upper line) and 0.5 m^{-1} (lower line) respectively.

Figs 9 and 10 show the effects of changing the important biological parameters. Decreasing the settling rate by a factor of ten resulted in somewhat more biomass, while a 4-fold increase in settling produced a greater decline in biomass (Fig. 9A).

The simulations were particularly sensitive to changes in the diatom respiration rate. Halving the rate (to r_{diatom} = 0.05) resulted in an earlier and much greater bloom, while an increase of 50% (to r_{diatom} = 0.15) meant the bloom did not occur at all (Fig. 9B). Setting both diatom and dinoflagellate respiration to 0.10 meant the bloom started earlier (late December), with surface biomass peaking at ~ 90 mg m^{-3} in mid-February, and then continuing as in Fig. 6. During the period of the bloom the average growth rates for r_{diatom} = 0.10 and r_{diatom} = 0.05 were similar (~ 0.4 d^{-1}). From eq. A1.7 it might have been expected that a lower respiration rate would produce a rather higher growth rate. However, the lower value of r_{diatom} meant more biomass was produced (Fig. 9B) so that self-shading increased. As a result lower r_{diatom} meant depth-averaged I, and thus depth-averaged P, were lower too, so the growth rate remained about the same.

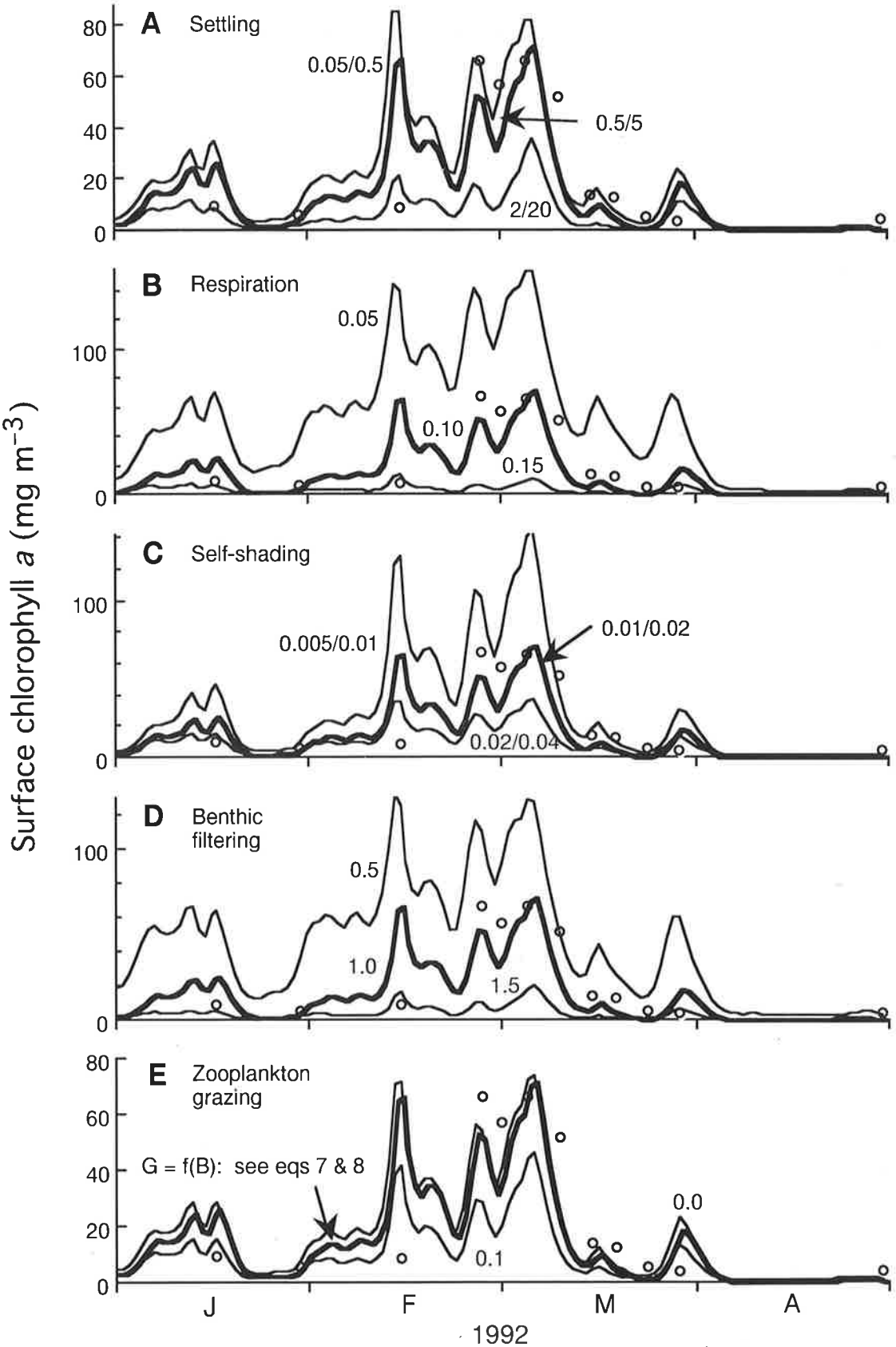

Figure 9 Effects on simulated biomass of varying certain biological parameters as follows: **A**, settling velocity ($w_{s,\text{smaller cells}}/w_{s,\text{larger cells}}$); **B**, diatom respiration as proportion of P_{max} (r_{diatom}); dinoflagellate respiration assumed constant at 0.35; **C**, phytoplankton self-shading ($k_{c,\text{larger cells}}/k_{c,\text{smaller cells}}$); **D**, benthic filtering (α); and **E**, zooplankton grazing (G). Parameters for the thick lines are given in Table 2, with alternative values noted on each of the other lines.

Fig. 9C shows the effects of halving or doubling the values of the self-shading coefficient (k_c) for the assemblages of larger and smaller cells. The bloom still occurred, but lower values of k_c produced higher simulated biomass, and vice versa.

Benthic grazing was another key factor. In the absence of grazing the bloom began in the middle of December, with biomass being ~ 200 mg m^{-3} in February–March, before declining by April. As grazing increased biomass declined (Fig. 9D), with no bloom occurring at $\alpha >$ 1.7 m d^{-1}. By contrast, the simulations were much less sensitive to zooplankton grazing. Fig. 9E shows the effect of varying G in the range 0–0.1 d^{-1}. For an assemblage dominated by diatoms, and relatively low values of B ($\geq$ 2.5 mg m^{-3}), G = 0.1 d^{-1} corresponds to higher values of F (eq. 8) than those calculated for the assumed composition and abundance of zooplankton in Manukau Harbour. For B in the range 5–50 mg m^{-3}, F is about 2–20 times higher than expected. Despite this higher zooplankton grazing, a bloom still occurred. And in the absence of grazing (G = 0 d^{-1}) biomass was only slightly higher than in the "best fit" simulation.

Fig. 10 shows how the simulations were affected by the composition of the phytoplankton assemblage. If dinoflagellates were never present and the only diatoms were smaller-sized, then biomass would have been high throughout the summer. By contrast, dinoflagellates, with their higher values of θ and r were unable to grow. Only with a lower respiration rate (r = 0.25) and substantially clearer water (k_x = 0.1 m^{-1}) did dinoflagellate-only simulations result in a bloom (with B reaching ~ 20 mg m^{-3} in December).

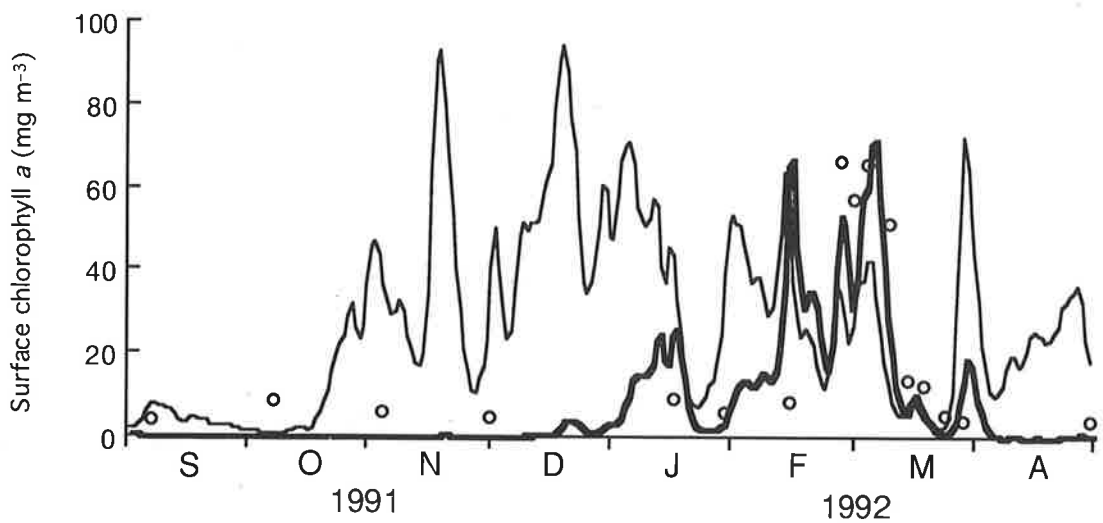

Figure 10 Effect of varying the composition of the phytoplankton assemblage. Thick line shows results obtained using observed proportions of diatoms and dinoflagellates to calculate community-average values of θ and r (assuming r_{diatom} = 0.10), while thin line is based on the assumption that the community was comprised solely of (small) diatoms.

DISCUSSION

These simulations suggest that the parameters which are important in determining the ability of phytoplankton to bloom in Manukau Harbour are:

- water depth (Fig. 7A);
- flushing (Fig. 7B);
- non-algal light attenuation (Fig. 8);
- phytoplankton respiration (Fig. 9B);
- benthic filtering (Fig. 9D); and
- phytoplankton community composition (Fig. 10).

Furthermore, it is clear that rather a lot of information on these parameters is required if reasonable simulations are to result. In particular, values are required for the following physiological characteristics of the phytoplankton community: light-saturated rate of photosynthesis (P_{max}), saturation onset PAR (I_k), self-shading coefficient (k_c), respiration as a proportion of P_{max} (r), cell carbon:chlorophyll *a* ratio (θ), and settling velocity (w_s). And all of these vary with time, either seasonally or as the composition of the phytoplankton assemblage shifts.

In many instances we have had to use literature values of these physiological parameters to estimate the likely values for the phytoplankton assemblage in Manukau Harbour. One interpretation of the "best fit" simulation shown in Fig. 6 is that these, and other unknown parameters, have been estimated satisfactorily. Alternatively, the effects of any errors may have cancelled each other. Regardless, it is noteworthy that relatively small changes in certain parameters (e.g., r, α) resulted in simulated levels of biomass which were markedly different from those measured. We cannot at present establish whether our assumed values for such parameters were correct, nor whether any short-term (e.g., diurnal) variation in them was minor (as we implicitly assume).

In highlighting the importance of such uncertainties, the model serves a valuable role in identifying where future studies are desirable. For example, studies of the benthic bivalve communities appear to be more important to our understanding of phytoplankton dynamics than studies of the zooplankton assemblage. Furthermore, the ease with which numerical experiments may be conducted is very useful in examining hypotheses and testing pre-conceived notions (e.g., does growth increase or decrease as respiration falls? would blooms be more likely if the benthic bivalves were decimated by over-harvesting or poisoning?).

Thus far the modelling has assumed that the harbour segments have a uniform cross-section (of depth H). However, respiration losses are undoubtedly greater in the channels than in the

better-lit intertidal area, while the opposite may be the case for losses to the bivalve grazers. It is not clear how important such differences between these habitats are. If the harbour waters are well-mixed horizontally over a time-scale which is similar to or shorter than that at which respiration- and grazing-induced losses become important, then it may be reasonable to ignore these differences. It would be worthwhile to examine this issue further, possibly extending the model to distinguish the intertidal and channel areas.

A related matter which also merits further attention concerns the fact that as the tide rises and falls over the intertidal zone, the area of well-lit waters must vary considerably. The underwater light climate and the associated phytoplankton photosynthesis will therefore be affected by the degree to which the rise and fall of the tide and the sun are in phase—which in Manukau Harbour varies from day-to-day over a fortnightly cycle.

The role of nitrogen and silicon in restricting growth should also be considered in the future. As observed earlier, inorganic nitrogen levels fell substantially during the bloom, presumably due to uptake by the rapidly-growing phytoplankton. As a result, simulations which produced extended periods of very high biomass (e.g., Fig. 8) are unlikely to be realistic. A useful extension of the model would therefore be to incorporate the parameters of nutrient uptake by phytoplankton. Such an extension would enable investigations to be made of the effects of possible reductions in harbour nutrient concentrations (e.g., following improvements in wastewater treatment).

ACKNOWLEDGEMENTS

D. S. Roper and R. D. Pridmore helped identify sources of information on the zooplankton and benthic bivalves. J. E. Hewitt ran numerical experiments with an earlier version of the model and checked all the algebra in Appendix 5. A. H. Ross made useful comments on a draft of this report.

REFERENCES

Asmus, R. M.; Asmus, H. 1991: Mussel beds: limiting or promoting phytoplankton? *Journal of experimental marine biology and ecology 148* : 215–232.

Baly, E. C. C. 1935: The kinetics of photosynthesis. *Proceedings of the Royal Society of London B 117* : 218–239.

Bannister, T. T. 1974: A general theory of steady state phytoplankton growth in a nutrient saturated mixed layer. *Limnology and oceanography 19* : 13–30.

Bioresearches 1987: Edible shellfish of the north-eastern Manukau Harbour. Report for Auckland Regional Authority Drainage Department.

Brenner, H. 1962: The diffusion model of longitudinal mixing in beds of finite length. Numerical values. *Chemical engineering science 17* : 229–243.

Brzezinski, M. A. 1985: The Si:C:N ratio of marine diatoms: interspecific variability and the effect of some environmental variables. *Journal of phycology 21*: 347–357.

Chan, A. T. 1980: Comparative physiological study of marine diatoms and dinoflagellates in relation to irradiance and cell size. II. Relationship between photosynthesis, growth, and carbon/chlorophyll *a* ratio. *Journal of phycology 16* : 428–432.

Cloern, J. E. 1982: Does the benthos control phytoplankton biomass in South San Francisco Bay? *Marine ecology progress series 9* : 191–202.

Cloern, J. E. 1991a: Tidal stirring and phytoplankton bloom dynamics in an estuary. *Journal of marine research 49* : 203–221.

Cloern, J. E. 1991b: Annual variations in river flow and primary production in the South San Francisco Bay Estuary (USA). *In* Elliott , M. & Ducrotoy, J.-P. (eds.) *Estuaries and Coasts: Spatial and Temporal Intercomparisons, ECSA19 Symposium.* Olsen & Olsen: 91–96.

Cloern, J. E.; Cole, B. E.; Wong, R. L.; Alpine, A. E. 1985: Temporal dynamics of estuarine phytoplankton: a case study of San Francisco Bay. *Hydrobiologia 129*: 153–176.

Cole, B. E.; Cloern, J. E. 1987: An empirical model for estimating phytoplankton productivity in estuaries. *Marine ecology progress series 36* : 299–305.

Deslou-Paoli, J.-M.; Lannou, A.-N.; Geairon, P.; Bougrier, S.; Raillard, O.; Heral, M. 1992: Effects of the feeding behaviour of Crassostrea gigas (bivalve molluscs) on biosedimentation of natural particulate matter. *Hydrobiologia 231*: 85–91.

Fee, E. J. 1990: Computer programs for calculating in situ phytoplankton photosynthesis. Canadian technical report of fisheries and aquatic sciences no. 1740. Department of Fisheries and Oceans, Winnipeg, 27 p.

Fischer, H. B.; List, E. J.; Koh, R. C. Y.; Imberger, J.; Brooks, N. H. 1979: *Mixing in inland and coastal waters.* New York: Academic Press.

Gallegos, C. L.; Platt, T. 1985: Vertical advection of phytoplankton and productivity estimates: a dimensional analysis. *Marine ecology progress series 26* : 125–134.

Geider, R. J.; Osborne, B. A. 1989: Respiration and microalgal growth: a review of the quantitative relationship between dark respiration and growth. *New phytologist 112*: 327–341.

Gray, W. G.; Pinder, G. F. 1976: An analysis of the numerical solution of the transport equation. *Water resources research 12* : 547–555.

Guymer, I.; West, J. R. 1988: The determination of estuarine diffusion coefficients using a fluorometric dye tracing technique. *Estuarine, coastal and shelf science 27* : 297–310.

Guymer, I.; West, J. R. 1991: Field studies of the flow structure in a straight reach of the Conwy estuary. *Estuarine, coastal and shelf science 32* : 581–596.

Herman, P. M. J.; Scholten, H. 1990: Can suspension-feeders stabilise estuarine ecosystems? *In:* Barnes, M.; Gibson, R. N. *eds.*, Trophic relationships in the marine environment, Proceedings of the 24th European marine biological symposium, pp. 104–116. Aberdeen University Press.

Hume, T. M. 1979: Aspects of the hydrology of the Mangere Inlet—Wairopa Channel area, northeast Manukau Harbour. Water and Soil Division, Ministry of Works and Development, Auckland, 62 p.

Jamart, B. M.; Winter, D. F.; Banse, K.; Anderson, G. C.; Lam, R. K. 1977: A theoretical study of phytoplankton growth and nutrient distribution in the Pacific Ocean off the northwest U.S. coast. *Deep-sea research 24* : 753–773.

Jassby, A. D.; Platt, T. 1976: Mathematical formulation of the relationship between photosynthesis and light for phytoplankton. *Limnology and oceanography 21* : 540–547.

Jillett, J. B. 1971: Zooplankton and hydrology of Hauraki Gulf, New Zealand. *New Zealand Oceanographic Institute memoir 53.*

Kirk, J. T. O. 1975: A theoretical analysis of the contribution of algal cells to the attenuation of light within natural waters. I. General treatment of suspensions of pigmented cells. *New phytologist 75*: 11–20.

Kirk, J. T. O. 1976: A theoretical analysis of the contribution of algal cells to the attenuation of light within natural waters. III. Cylindrical and spheroidal cells. *New phytologist 77*: 341–358.

Kirk, J. T. O. 1983: *Light and photosynthesis in aquatic ecosystems.* Cambridge, Cambridge University Press.

Lung, W.-S.; O'Connor, D. J. 1984: Two-dimensional mass transport in estuaries. *Journal of hydraulic engineering 110* : 1340–1357.

McBride, G. B. 1985: Incorporation of point sources in numerical transport schemes. *Water resources research 21* : 1791–1795.

McBride, G. B. 1992: Simple calculation of daily photosynthesis using five photosynthesis-light equations. *Limnology and oceanography 37* : 1796–1808.

McBride, G. B.; Cooke, J. G.; Donovan, W. F.; Hickey, C. W.; Mitchell, C.; Quinn, J. M.; Roper, D. S.; Vant, W. N. 1991: Residual flow and water quality studies for the Ararimu (Campbell Road) water supply scheme. Water Quality Centre Consultancy Report 6018, 57 p. Report to Auckland Regional Council (Operations Division).

Mallin, M. A.; Paerl, H. W. 1992: Effects of variable irradiance on phytoplankton productivity in shallow estuaries. *Limnology and oceanography 37* : 54–62.

Marra, J. 1978: Phytoplankton photosynthetic response to vertical movement in a mixed layer. *Marine biology 46* : 203–208.

Mason, M.; Weaver, W. 1924: The settling of small particles in a fluid. *Physics review 24* : 412–426.

Møhlenberg, F; Riisgård, H. U. 1979: Filtration rate, using a new indirect technique, in thirteen species of suspension-feeding bivalves. *Marine biology 54*: 143–147.

Ministry of Transport. 1990/1991: New Zealand Nautical Almanac 1990–91/1991–92. Government Printing Office Publishing, Wellington, New Zealand. 176/179 p.

Officer, C. B.; Smayada, T. J.; Mann, R. 1982: Benthic filter feeding: a natural eutrophication control. *Marine ecology progress series 9* : 203–210.

Park, J. K.; James, A. 1988: Time-varying turbulent mixing in a stratified estuary and the application to a Lagrangian 2-D model. *Estuarine, coastal and shelf science 27*: 503–520.

Parsons, T. R.; Takahashi, M.; Hargrave, B. 1984: *Biological oceanographic processes.* 3rd ed. Oxford, Pergamon Press, 330 p.

Platt, T.; Gallegos, C. L.; Harrison, W. G. 1980: Photoinhibition of photosynthesis in natural assemblages of marine phytoplankton. *Journal of marine research 38*: 687–701.

Platt, T.; Sathyendranath, S. in press: Estimators of primary production for interpretation of remotely-sensed data on ocean colour. *Journal of geophysical research (oceans).*

Platt, T.; Sathyendranath, S.; Ravindran, P. 1990: Primary production by phytoplankton: analytic solutions for daily rates per unit area of water surface. *Proceedings of the Royal Society of London, Series B 241*: 101–111.

Press, W. H.; Flannery, B. P.; Teukolsky, S. A.; Vetterling, W. T. 1986: *Numerical recipes, the art of scientific computing.* Cambridge, Cambridge University Press, 818 p.

Radach, G.; Moll, A. 1990: The importance of stratification for the development of phytoplankton blooms—a simulation study. *In:* Michaelis, W. *ed.*, Estuarine water quality management, *Coastal and estuarine studies 36*, pp. 389–394. Berlin, Springer-Verlag.

Smayda, T. J. 1970: The suspension and sinking of phytoplankton in the sea. *Oceanography and marine biology annual review 8*: 353–414.

Smith, E. L. 1936: Photosynthesis in relation to light and carbon dioxide. *Proceedings of the National Academy of Science 22* : 504–511.

Spiegel, M. R. 1968: *Mathematical handbook of formulas and tables.* New York, McGraw-Hill, 271 p.

Vant, W. N. 1991: Underwater light in northern Manukau Harbour, New Zealand. *Estuarine, coastal and shelf science 33* : 291–307.

Vant, W. N.; Budd, R. G. 1993: Phytoplankton photosynthesis and growth in contrasting regions of Manukau Harbour, New Zealand. *New Zealand journal of marine and freshwater research 27*: 295–307.

Vant, W. N.; Smith, D. G. 1991: Water quality effects of sewage effluent in the Manukau Harbour. *In:* Bell, R. G.; Hume, T. M.; Healy, T. R. *eds.*, Coastal engineering—climate for change, *Proceedings of 10th Australasian conference on coastal and ocean engineering*, pp. 307–312. Water Quality Centre Publication No. 21, Hamilton, New Zealand.

Vant, W. N.; Williams, B. L. 1992: Residence times of Manukau Harbour, New Zealand. *New Zealand journal of marine and freshwater research 26* : 413–424.

Varga, R. S. 1962: *Matrix iterative analysis.* New Jersey: Prentice-Hall, Englewood Cliffs.

Webb, W. L.; Newton, M.; Starr, D. 1974: Carbon dioxide exchange of *Alnus rubra*: a mathematical model. *Oecologia (Berlin) 17* : 281–291.

West, J. R.; Cotton, A. P. 1981: The measurement of diffusion coefficients in the Conwy estuary. *Estuarine, coastal and shelf science 12* : 323–336.

West, J. R.; Guymer, I.; Sangodoyin, Y.; Oduyemi, K. O. K. 1986: Solute dispersion and sediment transport in estuaries. *Water science and technology 18* : 93–100.

Winter, D. F.; Banse, K.; Anderson, G. C. 1975: The dynamics of phytoplankton blooms in Puget Sound, a fjord in the northwestern United States. *Marine biology 29* : 139–176.

Yotsukura, N. 1977: Derivation of solute-transport equations for a turbulent natural-channel flow. *Journal of research, U.S. Geological Survey 5* : 277–284.

NOMENCLATURE

Significant variables (M ≡ mass, L ≡ length, T ≡ time, E ≡ photon flux):

B chlorophyll *a* concentration, M L^{-3}
B_{sea} chlorophyll *a* concentration in the water beyond the harbour, M L^{-3}
$B_{G=0}$ chlorophyll *a* concentration at which zooplankton grazing ceases, M L^{-3}
c Courant number ($=w_s\Delta t/\Delta z$), dimensionless
D daylength (24 hours), h
F daily zooplankton ingestion rate, M T^{-1}
G specific zooplankton grazing rate, T^{-1}
H depth under the moving reference frame, L
I PAR, E M^{-2} T^{-1}
I_0 incident PAR, just below the water surface, E M^{-2} T^{-1}
I_k Saturation onset PAR, E M^{-2} T^{-1}
j node number, dimensionless
K_d vertical attenuation coefficient for PAR, L^{-1}
k_c self-shading coefficient, L^2 M^{-1}
k_x vertical attenuation coefficient for PAR in the absence of phytoplankton, L^{-1}
K_z vertical mixing coefficient for moving reference frame, L^2 T^{-1}
m mass of chlorophyll *a* in control volume, M
M mass of chlorophyll *a* in water column, M
n shape index for photoperiod PAR distribution, or time level; dimensionless
p $\mu - G - \xi/\Delta t_T$, T^{-1}
P instantaneous photosynthesis rate per unit biomass, T^{-1}
Q daily insolation, E M^{-2}
r respiration as a proportion of P_{max}, dimensionless
R mean daily tide range, L
t time, T
T doubling time, T
U mean daily wind speed, L T^{-1}
w_s settling velocity for phytoplankton, L T^{-1}
z depth under the moving reference frame, L
α specific benthic filtering rate, L T^{-1}
β benthic Courant number ($=\alpha\Delta t/\Delta z$), dimensionless
Δt time step, T
Δt_p photoperiod length, T
Δt_T tidal period (12 h 40 min), T
Δz grid distance interval, L
ζ optical depth ($=zK_d$), dimensionless
θ cell carbon:chlorophyll *a* ratio, dimensionless
ι PAR ratio ($=I/I_k$), dimensionless
μ net specific phytoplankton growth rate, T^{-1}
ξ tidal exchange coefficient, dimensionless
ρ function relating P to I, dimensionless
σ grid dispersion number ($=K_z\Delta t/\Delta z^2$), dimensionless
τ photoperiod fraction, dimensionless
Φ time since last spring tide, T
ϕ photoinhibition parameter, dimensionless
ω time-weight for numerical scheme, dimensionless

Appendix 1
CALCULATION OF DOUBLING TIMES

SUMMARY

The phytoplankton growth component of the model presented by Cloern (1991a) for South San Francisco Bay is based on a long incubation technique, and thus his model is based upon total cumulative PAR constant over 24 hours. In this case phytoplankton doubling times at the surface may be simply calculated. However calculation of doubling times is more difficult when using time-varying PAR (as we have used—we use short-term incubations), and/or depth-averages. This appendix describes how doubling rates can be calculated in numerical models. It also presents an analysis showing how doubling times can be calculated analytically, for both the Cloern and BLEST models (this excludes photoinhibition, though in principle it could be included).

This analysis shows that, using the Jassby-Platt photosynthesis-light equation with an exponential extinction of PAR down the water column and a sinusoidal variation of PAR through the photoperiod, the doubling time (T) averaged over depths greater than the euphotic depth is approximated by

$$T = \frac{\ell n(2)}{\mu_s\left[\dfrac{\delta(1.563 + 0.0767 I_{0,max}/I_k)}{Z} - r\right]}, \quad \text{provided that } 5 < \frac{I_{0,max}}{I_k} < 20$$

where: $\mu_s = P_{max}/\theta$ is the maximum specific phytoplankton growth rate in the absence of respiration; δ is the photoperiod day-fraction (the proportion of a day in sunlight); $I_{0,max}$ is the daily maximum PAR just below the water surface; I_k is the saturation onset parameter; $Z = zK_d$ is optical depth, where z = depth and K_d = vertical PAR attenuation coefficient; and r is the respiration proportion of the maximum growth rate. Generally $I_{0,max} < 5I_k$ only on very overcast days.

The minimum possible doubling time, which occurs for phytoplankton at the water surface in intense sunlight, is given by

$$T = \frac{\ell n(2)}{\mu_s(\delta - r)}, \quad \text{provided that } I_{0,max} >> I_k$$

DEFINITIONS

The doubling time for phytoplankton (T) is typically of the order of days. Therefore it is appropriate to use daily-average conditions when computing it. In doing so we must consider the specific phytoplankton growth rate (μ, as defined in eq. 3): doubling time is defined as the natural logarithm of 2 divided by the appropriate specific growth rate, i.e.,

$$T = \frac{\ell n(2)}{\mu^*} = \frac{0.69315}{\mu^*} \tag{A1.1}$$

where μ^* is a daily-average, and is either averaged over the water depth or is taken just under the water surface. To make clear what averaging is employed, and to be consistent with the main report, we follow the convention of McBride (1992) in which $<\mu>$ refers to depth-averaged growth rate, μ_T refers to daily-averaged growth rate ($_T$ refers to integration over *T*ime), and the subscript $_0$ refers to conditions just under the water surface.

If we expect substantial vertical mixing the depth-averaged specific growth rate is appropriate, so that $\mu^* = <\mu_T>$ in eq. A1.1, where

$$<\mu_T> = \frac{\int_0^H \left[\int_0^D \mu \, dt \right] dz}{HD} = \frac{\int_0^H \left[\int_0^D \frac{P_{max}}{\theta} (\rho - r) \, dt \right] dz}{HD} \tag{A1.2}$$

In this equation H = water depth; D = 1 day; μ = instantaneous specific phytoplankton growth rate; t = time since midnight; z = depth; P_{max} = maximum possible photosynthesis rate per unit biomass (i.e., growth is fully light-saturated); θ = the cell carbon to chlorophyll *a* ratio; $\rho = P/P_{max}$ is the "photosynthesis ratio" (McBride 1992), where P = instantaneous photosynthesis rate per unit biomass (so that $0 \le \rho \le 1$); and r = respiration proportion of P_{max}. If there is no photoinhibition ρ is a function only of the PAR ratio (ι), which is defined as (see also eq. 3):

$$\iota = \frac{I}{I_k} \tag{A1.3}$$

To compute ι at any depth we use the Beer-Lambert Law:

$$\iota = \iota_0 e^{-\zeta} \tag{A1.4}$$

where $\iota_0 = \frac{I_0}{I_k}$ and I_0 = PAR just under the water surface, I_k = saturation onset parameter (= $1/a$ in the terminology of Cloern 1991a, and assumed constant for a given species), and

$$\zeta = \int_0^z K_d(s)\, ds \tag{A1.5}$$

is the optical depth, with K_d = vertical PAR attenuation coefficient (see also eq. 5).

If vertical mixing is very slow it may be more appropriate to consider the daily-averaged phytoplankton doubling time at the water surface (T_0). This is obtained using the daily-averaged specific growth rate of phytoplankton at the water surface defined by:

$$\mu_{T,0} = \frac{\int_0^D \frac{P_{\max}}{\theta}(\rho_0 - r)\, dt}{D} \tag{A1.6}$$

where $\rho_0 = \rho(\iota_0)$. In this case $\mu^* = \mu_{T,0}$ in eq. A1.1.

From the above, to calculate T (or T_0), we must first calculate $<\mu_T>$ (or $\mu_{T,0}$) by prescribing the form of the variation of ρ with ι. For example, to use the Jassby-Platt *P-I* equation we must set $\rho = \tanh(\iota)$.

NUMERICAL CALCULATION OF DOUBLING TIMES

The numerical approximations to the required integrals (eqs A1.2 & A1.6) are obtained by substituting summations for the integrals. Accordingly we approximate eq. A1.2 by:

$$<\mu_T> \approx \frac{P_{\max}}{\theta}\left[\frac{\sum_{j=1}^{J}\sum_{n=1}^{N}\rho_j^n}{JN} - r\right] \tag{A1.7}$$

where J is the number of nodes in the vertical grid and N is the number of time steps in a day.

Similarly, eq. A1.6 becomes:

$$\mu_{T,0} \approx \frac{P_{\max}}{\theta}\left[\frac{\sum_{n=1}^{N}(\rho_0)^n}{N} - r\right] \tag{A1.8}$$

ANALYTICAL FORMS FOR CALCULATION OF DOUBLING TIMES

General form of the growth rate equations

It will be helpful to define the "fraction of photoperiod" (τ), as in eq. 4, i.e.,

$$\tau = \frac{t - t_{\text{sunrise}}}{\Delta t_p} \tag{A1.9}$$

where Δt_p ($= t_{\text{sunset}} - t_{\text{sunrise}}$) is the photoperiod. The photosynthesis ratio is nonzero only within the photoperiod (i.e., $\rho > 0$ only if $0 < \tau < 1$). However, $\rho = 0$ from midnight to sunrise ($\tau \leq 0$), and also from sunset to midnight ($\tau \geq 1$). This property, along with eqs A1.4 & A1.5, may be used to transform the equation for the daily- and depth-averaged specific phytoplankton growth rate (eq. A1.2) to the simpler form:

$$\langle \mu_T \rangle = \mu_s \left[\frac{\delta \langle \rho_T \rangle}{Z} - r \right], \quad \text{where} \quad \langle \rho_T \rangle = \int_0^1 \left(\int_0^Z \rho[\iota(\zeta,\tau)]\, d\zeta \right) d\tau \tag{A1.10}$$

where $\mu_s = P_{\max}/\theta$ is the maximum light-saturated specific growth rate in the absence of respiration, $\delta = \Delta t_p/D$ is the photoperiod day fraction (the fraction of the day in sunlight), $Z = HK_d$ is the optical depth at the bottom of the water column (K_d assumed constant with depth), and $\langle \rho_T \rangle$ is the dimensionless "daily water column photosynthesis ratio" (McBride 1992).

Also, the equation for the daily-averaged specific phytoplankton growth at the water surface (eq. A1.6) simplifies to:

$$\mu_{T,0} = \mu_s(\delta \rho_{T,0} - r), \quad \text{where} \quad \rho_{T,0} = \int_0^1 \rho[\iota_0(\tau)]\, d\tau \tag{A1.11}$$

where $\rho_{T,0}$ is a special case (i.e., surface value) of the dimensionless "daily photosynthesis ratio at a given depth" (McBride 1992).

The maximum possible value of the growth rate occurs at the surface when $\iota_0 >> 1$ throughout the photoperiod, so that $\rho \equiv \rho_T \equiv 1$ also. Then the growth rate is

$$\mu_{T,0,\max} = \mu_s(\delta - r) \tag{A1.12}$$

and the minimum possible doubling time is

$$T_{0,\min} = \frac{0.69315}{\mu_s(\delta - r)} \tag{A1.13}$$

Doubling times for constant PAR

As noted above the model presented by Cloern (1991a) holds incident PAR constant. In this case the growth rate equations (eqs A1.10 & A1.11) are simplified, because $\delta = 1$ and ρ is independent of τ (so that $\langle\rho_T\rangle = \langle\rho\rangle = \int_0^Z \rho\, d\zeta$, and $\rho_T = 1$).

As an example, let us consider Cloern's data: $H = 10$ m; $I_0 = 40$ Einst m^{-2} d^{-1}, $I_k = 10$ Einst m^{-2} d^{-1}, $K_d = k_x = 1.3$ m^{-1} (i.e., ignoring self-shading), $P_{max} = 100$ mg C (mg chl a)$^{-1}$ d^{-1}, $\theta = 50$ mg C (mg chl a)$^{-1}$, and $r = 0.05$. Therefore, $\mu_s = 2$ d^{-1}, $Z = 13$ and $\iota_0 = 4$. The Jassby-Platt P-I equation was used.

Surface doubling time

Computing the surface doubling time (T_0) is simple in this case. Inserting the above data into eq. A1.11 we obtain $\mu_{T,0} = 2[\tanh(4) - 0.05] = 1.90$ d^{-1}, and so, from eq. A1.1, $T_0 = 0.37$ days. The minimum possible surface doubling time, from eq. A1.13, is only slightly less—0.36 days.

Depth-averaged doubling time

Substituting Cloern's data into eqs A1.4 & A1.10 we obtain the depth-averaged growth rate as $\langle\mu_T\rangle = 2[\frac{\langle\rho_T\rangle}{13} - 0.05]$, where $\langle\rho_T\rangle = \int_0^{13}\tanh(4e^{-\zeta})d\zeta = \int_{4e^{-13}}^{4}\frac{\tanh(\xi)}{\xi}d\xi$. Computing this integral is tedious (McBride 1992, Table 5*). However that Table shows that a convenient solution can be obtained using the Smith P-I equation, which can be written in dimensionless form as

$$\rho = \frac{\iota}{\sqrt{1 + \iota^2}} \qquad \text{(A1.14)}$$

This can be expected to give results little different from the Jassby-Platt equation (McBride 1992). Substituting eqs A1.4 & A1.14 into the definition of $\langle\rho_T\rangle$ (eq. A1.10) we obtain

$$\langle\rho_T\rangle = \ell n\left(\frac{\iota_0 + \sqrt{\iota_0^2 + 1}}{\iota_Z + \sqrt{\iota_Z^2 + 1}}\right), \quad \text{where } \iota_Z = \iota_0 e^{-Z} \qquad \text{(A1.15)}$$

* It involves computing a partial fraction series with many terms, as shown in the Table—some 200 terms can be needed for convergence. Alternatively one can use an asymptotic solution (Spiegel 1968: eq. 14.612), but this may not be convergent.

and substituting this back into eq. A1.10 we have

$$<\mu_T> = \mu_s \left[\ell n \left(\frac{\iota_0 + \sqrt{\iota_0^2 + 1}}{\iota_Z + \sqrt{\iota_Z^2 + 1}} \right)^{1/Z} - r \right] \qquad \text{(A1.16)}$$

For a water column deeper than the euphotic depth ($Z = 4.6$) the denominator of the logarithm in this equation is approximately unity (because $\iota_Z \approx 0$) and so we can compute the doubling time for such depths as:

$$T_{Z>4.6} = \frac{0.69315}{\mu_s \left[\ell n \left(\iota_0 + \sqrt{\iota_0^2 + 1} \right)^{1/Z} - r \right]} \qquad \text{(A1.17)}$$

Using Cloern's data ($\mu_s = 2$ d^{-1}, $Z = 13$, $\iota_0 = 4$), $T_{Z=13} = 0.34657/\left[\ell n \left(4+\sqrt{17} \right)^{1/13} - 0.05 \right] = 3.12$ days. This result is an order of magnitude larger than the T_0 value obtained earlier, and this is attributable to the large aphotic depth (some 64% of the total depth). If we were to compute the doubling time only for the euphotic depth the result is T_{eu} ($= T_{Z=4.6}$) $= 0.34657/\left[\ell n \left(4 + \sqrt{17} \right)^{1/4.6} - 0.05 \right] = 0.86$ days.

Doubling times for time-varying PAR

Our incubations are short-term (3–4 hours), so the BLEST code allows for PAR varying with time. In order to get analytical solutions let us assume that I_0 varies as a half-sinusoid through the photoperiod, and so ι_0 varies similarly:

$$\iota_0 = \begin{cases} \iota_{0,max} \sin(\pi\tau) & 0 \le \tau \le 1 \\ 0 & \tau < 0 \text{ or } \tau > 1 \end{cases} \qquad \text{(A1.18)}$$

where $\iota_{0,max}$ is the PAR ratio just under the water surface at solar noon.*

In this section let us consider the data we used for the Manukau bloom (for 27 February 1992): $H = 3$ m, $P_{max} = 6.52$ mg C (mg chl a)$^{-1}$ h^{-1}, $\theta = 34.1$ mg C (mg chl a)$^{-1}$, $\Delta t_p = 12.9$ h, $r = 0.1$, $K_d = k_x = 1.85$ m^{-1} (i.e., ignoring self-shading), $I_k = 93.9$ µEinst m^{-2} s^{-1}, and daily 39

* Note that this is equivalent to taking the shape index of the daily PAR half sinusoid as $n = 1$, whereas we have used $n = 1.3$ in our modelling. This introduces an unknown error, which we nevertheless expect to be small. Also, BLEST allows K_d to be a function of depth.

ground-level PAR = 20.1 MJ m^{-2} d^{-1}. Therefore, μ_s = 6.52/34.1 = 0.191 h^{-1}, Z = 5.55, and δ = 12.9/24 = 0.54. We used the Jassby-Platt light equation.

To obtain $\iota_{0,max}$, ground-level PAR must be converted to $I_{0,max}$ and given the same units as I_k. The conversion factors are: 2.1 (converting MJ m^{-2} d^{-1} to Einst m^{-2} d^{-1}); 11.574 (converting Einst m^{-2} d^{-1} to μEinst m^{-2} s^{-1}); $0.5\pi/\delta$ (converting daily PAR to the maximum PAR in the photoperiod); and 0.95 (allowing a 5% loss of ground-level PAR by reflection at the water surface). So $I_{0,max}$ = 2.1x11.574x(0.5xπ/0.54)x0.95x20.1 ≈ 1356 μEinst m^{-2} s^{-1}, and thus $\iota_{0,max}$ = 1356/93.9 ≈ 14.4.

Surface doubling time

To compute $\mu_{T,0}$ we must substitute this time varying PAR ratio into the Jassby-Platt light function and substitute the result into eq. A1.11. As a result we must evaluate the integral $\rho_{T,0}$ = $\int_0^1 \tanh[\iota_{0,max}\sin(\pi\tau)]\, d\tau$, for which an analytical solution has not been found. There are two means of overcoming this difficulty.

The first is to note that a simple nomograph of ρ_T versus ι_{max} is available McBride (1992: Fig. 4). This was obtained by numerical integration, and we can use it to read the value of ρ_T for a given value of ι_{max} (actually $\iota_{0,max}$ in this case, as our "depth" is zero). So using $\iota_{0,max}$ = 14.4, we read that for the Jassby-Platt equation $\rho_{T,0} \approx 0.97$, and so eq. A1.11 gives $\mu_{T,0}$ = 0.191(0.54x0.97–0.1) = 0.081 h^{-1}. From eq. A1.1 this corresponds to a doubling time of 0.36 days. (Coincidentally, this is nearly the same surface doubling rate as was calculated for South San Francisco Bay.)

The second approach again uses the Smith equation (eq. A1.14). We also use the result from McBride (1992: Table 4), that for the Smith equation

$$\rho_T = \frac{2}{\pi}\sin^{-1}(\Psi), \quad \text{where } \Psi = \frac{\iota_{0,max}}{\sqrt{1+\iota_{0,max}^2}} \qquad \text{(A1.19)}$$

Equation A1.11 is then transformed to

$$\mu_{T,0} = \mu_s\left[\frac{2\delta}{\pi}\sin^{-1}(\Psi) - r\right] \qquad \text{(A1.20)}^*$$

---

* For $\iota_{0,max} >> 1$, $\sin^{-1}(\Psi) \rightarrow \sin^{-1}(1) = \frac{\pi}{2}$, and so eq. A1.20 collapses to eq. A1.12, as required.

Note that for our Manukau Harbour data $\Psi = 14.4/\sqrt{1+14.4^2} = 0.9976$, so we compute that $\mu_{T,0} = 0.191\{[2x0.54x\sin^{-1}(0.9976)]/\pi - 0.1\} = 0.079\ h^{-1}$, corresponding to a doubling time of 0.37 days. This is little different from the first approach.

From eq. A1.13 the minimum possible doubling time is 0.35 days.

Depth-averaged doubling time

To compute $<\mu_T>$ we must substitute eqs A1.4 & A1.18 into the Jassby-Platt light function and substitute the result into eq. A1.10. Once again, analytical solutions for the Jassby-Platt equation cannot be found, and again we present two methods of overcoming this difficulty.§

The first is to use the nomographs of $<\rho_T>$ versus $\iota_{0,max}$ for the Jassby-Platt equation presented by McBride (1992, Fig. 5d). For $\iota_{0,max} = 14.4$ and $Z = 5.55$ we get $<\rho_T> \approx 2.7$. Therefore eq. A1.10 gives $<\mu_T> = 0.191[(0.54x2.7)/5.55 - 0.1] = 0.031\ h^{-1}$, corresponding to a depth-averaged doubling time of 0.93 days—very similar to that obtained above for the South San Francisco Bay doubling time averaged over the euphotic depth (note that for Manukau Harbour $Z = 5.55$, which is approximately the euphotic depth).

The second approach follows that of Platt & Sathyendranath (in press). They noted that whereas models of daily water column photosynthesis give a nonlinear function of PAR (as the nomographs in McBride 1992 demonstrate), field observations often show a linear dependence on PAR (e.g., Cole & Cloern 1987, Cloern 1991b, Vant & Budd 1993). They resolved this difference by noting that for values of PAR of practical interest, only a weak curvature actually occurs in the model solutions. They then identified some simple linear functions relating $<\rho_T>$ (their f) versus $\iota_{0,max}$ (their I_m^*) for deep water (corresponding to $\zeta \gtrsim 5$). In particular for a wide range of PAR ($3 \le \iota_{0,max} \le 20$) they found $<\rho_T> = 1.23 + 0.0910\iota_{0,max}$; for $3 \le \iota_{0,max} \le 20$, they found the more accurate approximation $<\rho_T> = 0.940 + 0.1390\iota_{0,max}$. A similar approach is followed here for the Jassby-Platt equation.

We use the $Z = 5$ curve on Fig. 5d of McBride (1992), because it corresponds to the water depth for the Manukau Harbour, and also is little different from the euphotic depth. Selecting data for that curve for $5 < \iota_{0,max} < 22$, linear regression gives $<\rho_T> \approx 1.563 + 0.0767\iota_{0,max}$ (adjusted $r^2 = 0.95$). Therefore, for $\iota_{0,max} = 14.4$, $<\rho_T> \approx 2.6$, and so $<\mu_T> = 0.030$ and the depth-averaged doubling time is 0.97 days.

---

§ We have found an asymptotic series solution for the Smith equation (using eq. 14.346 of Spiegel 1968), but its convergence is not satisfactory (it contains Bernoulli numbers which get very large for later terms in the series). Platt *et al.* (1990) present a series solution for the *P-I* equation of Webb et al. (1974) ($\rho = 1 - e^{-\iota}$) for the infinite-depth case, which gives very similar results to those obtained with the Jassby-Platt and Smith equations. They also present a very accurate 5-term polynomial approximation to it, and show how photoinhibition may be included (i.e., using the *P-I* equation of Platt *et al.* 1980).

This approximate approach gives results little different from that using the nomograph. Its general form may therefore be of some use, i.e.,

$$T = \frac{\ell n(2)}{\mu_s\left[\frac{\delta(1.563 + 0.0767 t_{0,max})}{Z} - r\right]}, \text{ provided that } 5 < t_{0,max} < 20 \qquad \text{(A1.21)}$$

Appendix 2
FEE'S INCIDENT PAR CALCULATION PROCEDURE

Using Fee's terminology, the procedure for calculating the daily PAR variation at Hobsonville on 8 February 1992 is as follows:

Physical data

θ	= –36.8°	= "LATITUDE";
d	= 39	= day number of year;
λ_y	= 366	= number of days in year;
ϕ	= –15.5153°	= 23.45°sin[360°(284+39)/365] = declination of the earth;
φ	= 101.9865°	= arccos[–tan(θ)tan(ϕ)] = angle from due south of the sun at sunset;
λ_d	= 815.8916 min	= 8φ = "daylength", i.e., photoperiod;
k	= 38.4658°	= 360°d/λ_y = day angle;
δ_s^2	= 1.0276	= 1.00011 + 0.034221 cos(k) + 0.001280 sin(k) – – 0.000719 cos(2k) + 0.000077 sin(2k), the square of the earth's deviation from its mean distance from the sun;
Θ	= 373.4 mE m^{-2} min^{-1}	= solar constant.

The values of these variables are all fixed for a given site and time.

Empirical data

κ_a	= 0.3608	= "ATMOS_EFFECT" = fraction of PAR at the top of the atmosphere reaching the water surface, determined from the inspected PAR maximum and Fee's "FITSOLAR" routine. This is the only empirical variable that the user can adjust.

Incident PAR Formula

$$I_0(t) = \kappa_a \Theta \delta_s^2 \{\sin(\phi)\sin(\theta) + \cos(\phi)\cos(\theta)\cos[0.25°(t-\lambda_d/2)]\} \quad \text{(A2.1)}$$

where t is time from sunrise in minutes ($0 \le t \le \lambda_d$), and I_0 is in mEinst m^{-2} min^{-1}. Converting t to time since midnight in hours (as on Fig. 4), converting Θ to µEinst m^{-2} s^{-1}, and substituting the above values for κ_a, Θ, δ_s^2, ϕ, θ and λ_d into eq. A2.1 we obtain the formula used to generate the Fee curve (a regular sinusoid) on Fig. 5:

$$I_0(t) = 2307.35\{0.1602 + 0.7716 \cos[15(t-5.75)-101.9865]\},\ \mu\text{Einst } m^{-2}\ s^{-1}.$$

Appendix 3
BLEST DIFFERENCE EQUATIONS

Mass balances of phytoplankton (of concentration B) are applied to the control volumes shown on the figure. The (constant) settling velocity is w_s, and the specific benthic uptake rate is α.

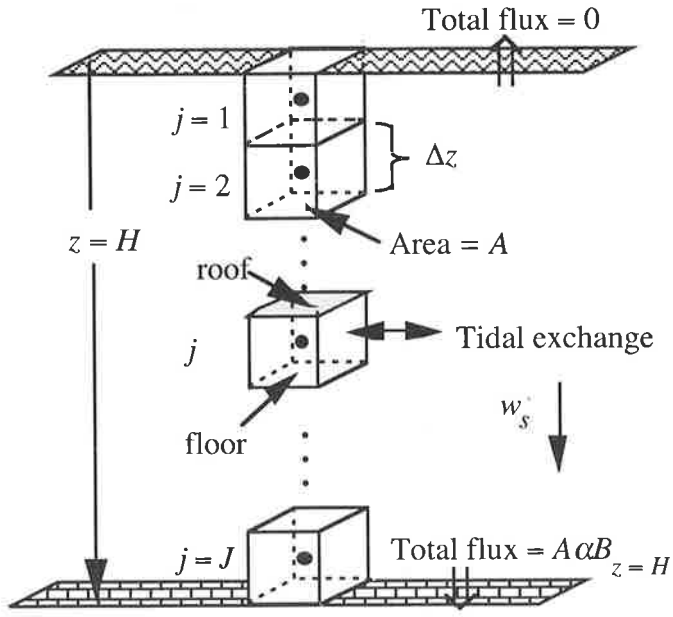

Each control volume has a centroid node, labelled j, and they all have horizontal surface area = A and volume $A\Delta z$. The mass balances are written for a time interval Δt ($= t^n - t^{n-1}$).

An Eulerian frame of reference is used in the vertical direction, because the system is diffusion-dominated (the settling velocity can be expected to be much lower than the vertical diffusion velocity). In contrast, a Lagrangian frame of reference is used in the horizontal direction, to allow for movement of the control volumes up and down the estuary as the tide ebbs and flows.

The mass balance equation for the general control volume j is thus:

mass in volume j at time t^n – mass in volume j at time t^{n-1}
= mass advected and diffused through the roof in time Δt
– mass advected and diffused through the floor in time Δt
+ net mass produced/grazed/respired in the volume in time Δt
– net mass lost by exchange with surrounding waters in time Δt (A3.1)

The mass in a control volume at any time is taken as the volume times the concentration at the centroid (i.e., $\text{mass}_j = A\Delta z B_j$). The rate of advection of mass through the roof is taken as $Aw_s B_{\text{roof}}$, and similarly for the floor. If we use a Fickian description of diffusion, the rate of

diffusion of mass through the roof is $[-AK_z(\partial B/\partial z)]_{\text{roof}}$, and similarly for the floor. To obtain the mass advected or diffused through the roof or floor during Δt, the respective rates are multiplied by Δt and referred to some time level between t^n and t^{n-1} (denoted by an asterisk). Accordingly, the algebraic form of the mass balance equation for control volume j is:

$$\begin{aligned} AB_j^n\,\Delta z - AB_j^{n-1}\Delta z \;&= \{Aw_sB^*\Delta t + [-AK_z\frac{\partial B}{\partial z}]^*\Delta t\}_{\text{roof}} \\ &- \{Aw_sB^*\Delta t + [-AK_z\frac{\partial B}{\partial z}]^*\Delta t\}_{\text{floor}} \\ &+ A[S_j^* + GB_{G=0} + \xi B_{\text{sea}}/\Delta t_T]\Delta z\Delta t \end{aligned} \tag{A3.2}$$

where Δt_T is the tidal cycle (from high tide to high tide) and S is the net internal rate of gain of mass per unit control volume per unit time. Because S is first-order we have $S = pB$, where $p(z,t)$ is the net specific growth rate. From eq. 9 we see that $p = \mu - G - \xi/\Delta t_T$.

It is now necessary to make three approximations. First, we use the time-weighting approximation:

$$X^* = \omega X^n + \bar{\omega}X^{n-1}\ , \text{ such that } 0 \le \omega \le 1 \text{ and } \bar{\omega} = 1 - \omega \tag{A3.3}$$

where X denotes any of the quantities (B, $\partial B/\partial z$, or S) to be evaluated at time level *. Second, to evaluate B at the roof or floor we take the linear interpolation functions:

$$B_{\text{roof}} = (B_j + B_{j-1})/2 \text{ and } B_{\text{floor}} = (B_{j+1} + B_j)/2 \tag{A3.4}$$

Finally, to evaluate the derivatives we take:

$$(\partial B/\partial z)_{\text{roof}} = (B_j - B_{j-1})/\Delta z \text{ and } (\partial B/\partial z)_{\text{floor}} = (B_{j+1} - B_j)/\Delta z \tag{A3.5}$$

Substituting eqs. A3.3–A3.5 into eq. A3.2, noting that $S = pB$, and dividing by the control volume ($A\Delta z$):

$$\begin{aligned} &\omega(-c/2 - \sigma^n)B_{j-1}^n + [1+\omega(2\sigma^n - p_j^n\Delta t)]B_j^n + \omega(c/2 - \sigma^n)B_{j+1}^n = \\ &\bar{\omega}(c/2 + \sigma^{n-1})B_{j-1}^{n-1} + [1 + \bar{\omega}(-2\sigma^{n-1} + p_j^{n-1}\Delta t)]B_j^{n-1} + \bar{\omega}(-c/2 + \sigma^{n-1})B_{j+1}^{n-1} \\ &+ (GB_{G=0} + \xi B_{\text{sea}}/\Delta t_T)\Delta t \end{aligned} \tag{A3.6}$$

for $j = 2,\ldots, J-1$, where c $(= w_s\Delta t/\Delta z)$ is the Courant number and σ^n $(=K_z^n\,\Delta t/\Delta z^2)$ is the grid dispersion number.

This equation applies only to the interior control volumes (i.e., $j = 2,..., J-1$). For the top control volume ($j = 1$) the surface boundary condition must be applied to its roof. Likewise, for the bottom control volume ($j = J$) the bottom boundary condition must be applied to its floor.

Surface boundary condition

This condition, i.e., $-AK_z(\partial B/\partial z)_{z=0} + (Aw_s B)_{z=0} = 0$, is incorporated into the difference equation for the first control volume by setting the first term on the right-hand-side of eq. A3.2 to zero. The resulting equation is:

$$\begin{aligned}&[1+ \omega(c/2 + \sigma^n - p_1^n\Delta t)]B_1^n \quad + \quad \omega(c/2 - \sigma^n)B_2^n \;=\\ &[1 + \bar{\omega}(-c/2 - \sigma^{n-1} + p_1^{n-1}\Delta t)]B_1^{n-1} \;+\; \bar{\omega}(-c/2 + \sigma^{n-1})B_2^{n-1}\\ &+ [GB_{G=0} + \xi B_{\text{sea}}/\Delta t_T]\Delta t\end{aligned} \tag{A3.7}$$

Bottom boundary condition

Here the total mass leaving the boundary through Δt is $A\alpha B^*_{z=H}\Delta t$. Accordingly, the equation for control volume J is obtained by replacing the second term on the right-hand-side of eq. A3.2 by $A\alpha B^*_J\Delta t$. In doing so, to be consistent with the linear interpolation approximations made for interior control volumes (i.e., eq. A3.4), we use a linear extrapolation for $B_{z=H}$:

$$B_{z=H} = (3B_J - B_{J-1})/2 \tag{A3.8}$$

The resulting equation for control volume J is:

$$\begin{aligned}&\omega(-c/2 - \sigma^n - \beta/2)B_{J-1}^n \;+\; [1+ \omega(-c/2 + \sigma^n + 3\beta/2 - p_J^n\Delta t)]B_J^n \;=\\ &\bar{\omega}(c/2 + \sigma^{n-1} + \beta/2)B_{J-1}^{n-1} \;+\; [1 + \bar{\omega}(c/2 - \sigma^{n-1} - 3\beta/2 + p_J^{n-1}\Delta t)]B_J^{n-1}\\ &+ [GB_{G=0} + \xi B_{\text{sea}}/\Delta t_T]\Delta t\end{aligned} \tag{A3.9}$$

where $\beta = \alpha\Delta t/\Delta z$ (a kind of benthic Courant number).

Calculating PAR at depth

Calculation of the specific phytoplankton growth rate at any time or depth, from eq. 3, requires the value of the PAR ratio (ι). Calculation of this ratio, from eq. 5, must account for the nonlinear effect of self-shading. This nonlinearity is avoided in the numerical scheme by evaluating B in the self shading term at the old time-level, $n-1$. Accordingly the BLEST equations for the PAR ratio are:

$$(\iota_0)_1^n \;=\; (\iota_0)^n_{\text{surface}}\, \exp[-k_x - k_c B_1^{n-1}/2] \tag{A3.10}$$

and

$$(\iota_0)_j^n = (\iota_0)_{j-1}^n \exp[-k_x - k_c(B_j^{n-1} + B_{j-1}^{n-1})/2] \qquad \text{(A3.11)}$$

for $j = 2,..., J$.

Assembling the scheme equations

For any time level the scheme (i.e., eqs. A3.6, A3.7 and A3.9) can be assembled into the matrix form $\mathbf{Ax} = \mathbf{f}$, where $\mathbf{x}$ is a column vector of the unknowns $(B_1^n\ B_2^n\ ...\ B_J^n)^T$ and $\mathbf{f}$ is a column vector of the known (i.e., at the $n-1$ time level) right-hand-sides of the scheme equations. $\mathbf{A}$ is a square (J x J) tridiagonal matrix containing the coefficients on the left-hand sides of the scheme equations [e.g., for an interior control volume the subdiagonal, diagonal and superdiagonal terms are: $\omega(-c/2 - \sigma^n)$, $1+ \omega(2\sigma^n - p_j^n\Delta t)$, and $\omega(c/2 - \sigma^n)$ respectively]. This equation may be solved very efficiently for B_j^n ($j = 1,..., J$) by a standard Gaussian elimination algorithm (we used subroutine TRIDAG of Press *et al.* 1986). This algorithm is stable so long as the matrix is diagonally dominant, generally requiring only that $\omega\, p_j^n \Delta t < 1$. However, it is well-known that stability problems may arise for $\omega < 0.5$.

Appendix 4
TESTING THE MODEL'S ACCURACY

Testing is necessary to ensure that the model code is free from programming errors, and that it produces results of acceptable accuracy. This takes three forms: examination of whether the model conserves mass (of phytoplankton); the match between the model's predicted concentrations and those obtained with an available analytical solution; and a simple exponential growth bloom.

In the first two cases we are constrained to ignoring phytoplankton growth and losses (i.e., $\mu = G = \xi = 0$ in eq. 9), because only then is mass preserved. Also, analytical results are generally only available for this case. Although such testing ignores blooms, it is nevertheless very instructive because the major approximation errors may be expected to occur in the modelling of advection, dispersion and the incorporation of boundary conditions.

We used results at the end of the 14th day of simulation, thus allowing sufficient time for any errors to become obvious. Water depth was set at H = 10 m, time-step Δt = 0.1 d, and grid distance interval Δz = 0.1 m. Settling velocity and the vertical mixing coefficient were varied from w_s = 0–0.5 m d^{-1} and K_z = 0–5 m^2 d^{-1} respectively, following values used by Cloern (1991a).

Mass conservation tests

In the mass conservation tests the benthic flux was set to zero ($\alpha = 0$). An algebraic analysis for this case shows that BLEST should conserve mass *exactly* (see Appendix 5). (While the concentrations predicted by numerical schemes are indeed approximate, errors in the overall mass conservation cannot be tolerated.) The four possible cases are shown in Table A4.1, along with the computed mass balance errors. All tests used an arbitrary initial concentration of B_i = 500 mg m^{-3}.

TABLE A4.1 Mass balance test cases and errors

Case	Data		Mass balance error
	w_s, K_z §	ω #	
(a) Stagnant water	0, 0	0.5	0
(b) Pure diffusion	0, 5	0.5	4 x 10^{-16}
(c) Pure advection	0.5, 0	0.5, 1.0	2 x 10^{-15}
(d) Advection-diffusion	0.5, 5	0.5	3 x 10^{-14}

§ corresponding to c = 0.5 (Courant no.), σ = 50 (dispersion no.)
# ω = time-weight, dimensionless

The table shows that any mass balance error is minimal. It is the result of rounding errors in the way the computer stores numbers. The actual concentrations calculated at cell floors are given on Fig. A4.1.

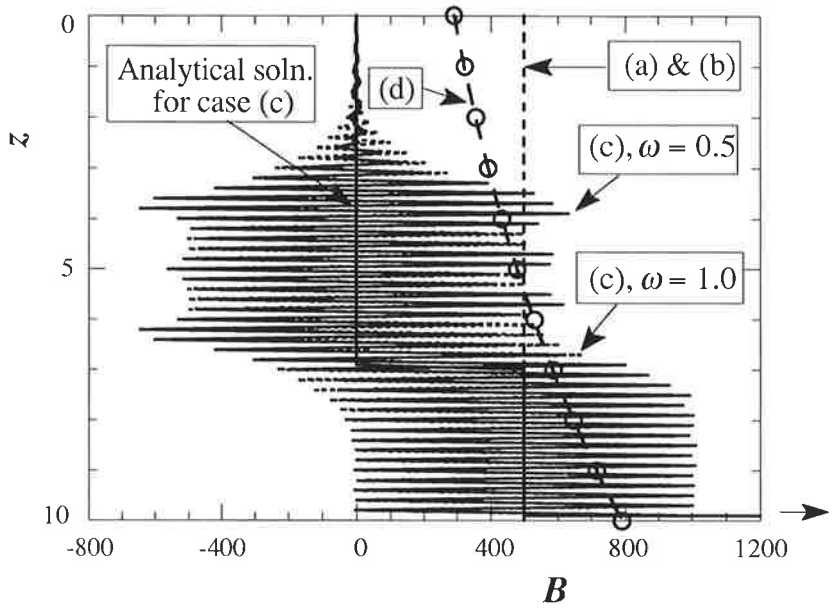

Figure A4.1 Mass conservation tests
[data given on Table A4.1, circles show analytical solution for case (d)]

For cases (a) and (b) the model preserves the initial condition, as expected. Case (c) (pure advection) presents a severe test to any numerical scheme, because of the presence of two sharp fronts of concentration. The first is at 7 m depth, where B jumps from 0 to 500 mg m^{-3}, and the second is at the bed (at 10 m), where rapid accumulation of B occurs. Wildly oscillatory (but stable) results are obtained, with $\omega = 0.5$ being generally more noisy than $\omega = 1.0$ ($\omega = 0.5$ is "time-centring", as in the Crank-Nicolson scheme used by Cloern 1991a, $\omega = 1$ gives the "fully-implicit" scheme). Both time-weightings give very large concentrations ($B \approx 134{,}500$) at the bed (where the analytical solution becomes infinite). Note that these are cell floor values which are obtained by interpolation between nodal values (eq. A3.4), and extrapolation to the bed (eq. A3.8). (The nodal concentrations oscillate with an amplitude that increases almost linearly from 0 at $Z = 2.8$ m to 72 750 at $Z = 9.95$ m.)

It is well-known that the Crank-Nicolson scheme is oscillatory when modelling pure advection of steep concentration gradients (e.g., Gray and Pinder 1976). It is less well-known that it, and the fully-implicit scheme, become even more oscillatory in the presence of a *fixed* steep concentration gradient (i.e., at the bed) (see also McBride 1985).

Case (c) is of course not physically realistic, because it ignores dispersion. Case (d) shows that when modest dispersion is included the results obtained contain no noise. These results are also very accurate (as discussed below).

Analytical solution tests

The noisy solutions obtained near the bed in the pure advection case (c) above are the result of attempting to resolve a huge concentration gradient. This gradient can be removed by allowing phytoplankton to pass through the bed at the same rate that it is advected downward. This is achieved by setting the specific benthic filtering rate to the settling velocity, i.e., $\alpha = w_s$ (this equates the Courant numbers for the water and the bed, i.e., $c = \beta$). The (step-function) analytical solution is known for this case, and is shown with the BLEST results on Fig. A4.2.

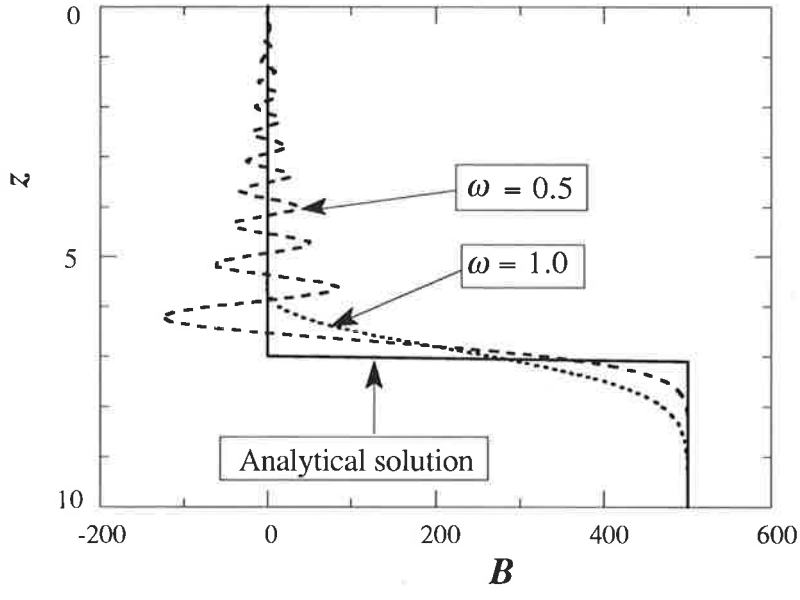

Figure A4.2 Analytical and BLEST solutions for pure advection
($\alpha = w_s = 0.5$ m d^{-1}, $K_z = 0$ m^2 d^{-1})

These results are now correct at the bed. They do show some smearing of the sharp front, and the Crank-Nicolson scheme (i.e., $\omega = 0.5$) results also show oscillations above it. These are as expected from these schemes. However, as we have noted, this is a severe test of the scheme, because some dispersion is always present. An analytical solution for the appropriate case including dispersion has been found. This considers the advection/dispersion of phytoplankton with a nonzero initial condition subject to there being no mass flux through the water surface, and no gradient of phytoplankton at the bed (so that there is only advective flux through the bed). The equations for this problem are:

$$\frac{\partial B}{\partial t} + w_s \frac{\partial B}{\partial z} = K_z \frac{\partial^2 B}{\partial z^2} \tag{A4.1}$$

with the initial condition $B(z,0) = B_i$ and the boundary conditions $(w_s B - K_z \frac{\partial B}{\partial z})_{z=0} = 0$ and $(\frac{\partial B}{\partial z})_{z=H} = 0$. An approximate, but nevertheless accurate analytical solution is (Brenner 1962):

$$\frac{B}{B_i} = 1 - \frac{1}{2}\mathrm{erfc}\left[\sqrt{\frac{P}{T}}(Z-T)\right] - \sqrt{\frac{4PT}{\pi}}\, e^{-P(Z-T)^2/T} + \frac{1}{2}[1 + 4P(Z+T)]\, e^{4PZ}\, \mathrm{erfc}\left[\sqrt{\frac{P}{T}}(Z+T)\right] \tag{A4.2}$$

where $Z = z/H$ is dimensionless depth, $T = w_s t/H$ is dimensionless time, $P = w_s H/(4K_z)$ is the Péclet number, and erfc is the complementary error function [$\mathrm{erfc}(x) = \frac{2}{\sqrt{\pi}}\int_x^\infty e^{-\xi^2}\, d\xi$]. This solution was implemented using ERFC and associated functions in Press *et al.* (1986).

Fig. A4.3 demonstrates a comparison between the numerical solution obtained by the BLEST code (using $\omega = 0.5$) and the analytical solution obtained from eq. A4.2. The input data were selected so that there is a negligible gradient at the bed—if not eq. A4.2 would be invalid. The agreement between the two solutions is excellent. Inspection of the data files show that for these input data the difference between the two solutions is never more than 0.13%.

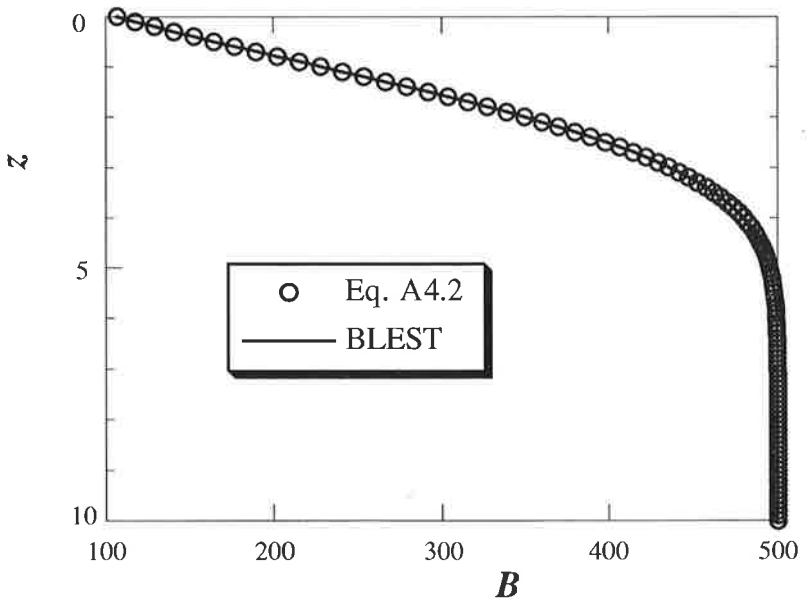

Figure A4.3 Analytical & BLEST advection/dispersion solutions

($\alpha = w_s = 0.1$ m d^{-1}, $K_z = 0.1$ m^2 d^{-1})

Finally, note that Fig. A4.1 (case d) shows similarly accurate solutions for the case where no mass is permitted to enter or leave either boundary (i.e., $w_s B - K_z \frac{\partial B}{\partial z} = 0$ at $z = 0$ and H). The analytical solution for this case seems to be even less known than that of Brenner (1962). It was derived by Mason & Weaver (1924, their eq. 14'), and is:

$$\frac{B}{B_i} = \frac{e^{Z/\lambda}}{\lambda(e^{1/\lambda}-1)} + 16\lambda^2\pi e^{P(2Z-T)} \sum_{m=1}^{\infty} \frac{e^{-\lambda m^2\pi^2 T} m(1 \pm e^{-1/(2\lambda)})(\sin m\pi Z + 2\pi m\lambda \cos m\pi Z)}{(1 + 4\pi^2 m^2 \lambda^2)^2} \quad \text{(A4.3)}$$

with P, T and Z defined as for eq. A4.2, and $\lambda = \frac{1}{4P}$.§ The top sign (in the $\pm$ term) is taken if m is odd, the lower is taken if m is even. Two terms are generally sufficient, unless t and K_z are both small.

Bloom tests

Here vertical settling and dispersion and benthic flux were set to zero, and the source term was set to a constant value, $p\Delta t = 0.1\Delta t$. Then after 14 days the analytical solution is $B = 500e^{+1.4} = 2027.59998$. Using double precision in the code we obtained extremely accurate results for a time-weight $\omega = 0.5$ (result 2027.62364). For $\omega = 0.0$ or 1.0 the results were a little less accurate (2013.55 and 2041.94). This is to be expected, as we can show that $\omega = 0.5$ corresponds to a second-order accurate Padé approximant for the exponential function (e.g., Varga 1962), whereas other values of ω are only first-order accurate.

Which time weight?

From the above, $\omega = 1.0$ is the most accurate if steep fronts of concentration are present, whereas $\omega = 0.5$ is the most accurate for a bloom. As steep fronts are not anticipated, we use $\omega = 0.5$.

---

§ There are two typographical errors in Mason & Weaver's paper.
(i) In their eq. 15 they define $y = Lx$ (equivalent to $Z = Hz$ in our nomenclature): it should be $y = x/L$ (i.e., $Z = z/H$, as defined for our eq. A4.2).
(ii) There is a minus sign missing from the first summed exponential in their dimensional solution (eq. 14).

Appendix 5
MASS CONSERVATION OF NUMERICAL SCHEMES

BLEST control-volume scheme

Nodes (j = 1, ..., J) are placed at the centroids of control volumes, so there are no nodes at the boundaries. Boundary conditions are incorporated into the scheme by prescribing the mass-flux through the roof of the 1st control-volume, and through the floor of the J^{th} control-volume.

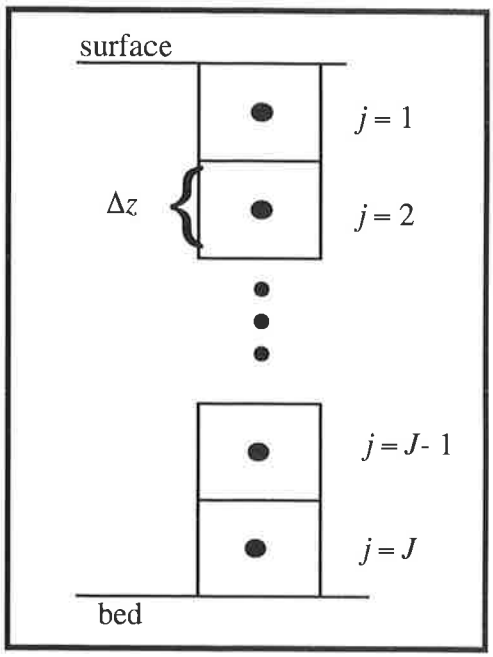

Take the case of a conservative solute, with zero mass-transport through the estuary bed (so $\mu = G = \alpha = \xi = 0$). The mass in the water column at one time level should be exactly the same as at the previous level, i.e.,

$$M^n = M^{n-1} \qquad \text{(A5.1)}$$

This must be true for *any* values of vertical diffusivity (K_z) and settling velocity (w_s). In our control-volume scheme this is guaranteed. To see this, note that

$$M^n = \Sigma AB_j^n \Delta z = \Sigma m_j^n \qquad \text{(A5.2)}$$

where Σ denotes summation from j = 1 to J. We can summarise eqs. A2.1 and A2.2 as:

$$m_j^n - m_j^{n-1} = (m_j)^*_{\text{roof}} - (m_j)^*_{\text{floor}} \qquad \text{(A5.3)}$$

and

$$(m_j)^*_{\text{floor}} = (m_{j+1})^*_{\text{roof}} \qquad \text{(A5.4)}$$

Therefore

$$\Sigma m_j^n = \Sigma m_j^{n-1} + (m_1)^*_{\text{roof}} - (m_J)^*_{\text{floor}} \qquad \text{(A5.5)}$$

All internal fluxes cancel *exactly*, as required. Also, our boundary conditions specify that $(m_1)^*_{\text{roof}} = (m_J)^*_{\text{floor}} = 0$. Hence eq. A5.5 collapses to eq. A5.1, and mass conservation is satisfied exactly.

Cloern's finite difference scheme

In this scheme (described briefly in Cloern 1991a), nodes are placed *at* the boundaries ($i = 1$ and $i = I$). For the internal nodes ($i = 2, ..., I–1$) the scheme is identical to the time-centred control-volume scheme (i.e., eq. A3.6 with $\omega = 1/2$, and $j = i$). However, boundary conditions were applied in an *ad hoc* way, directly to the boundary nodes, without requiring mass conservation in the half volumes containing those nodes. As a result the whole scheme falsifies mass. We show this as follows.

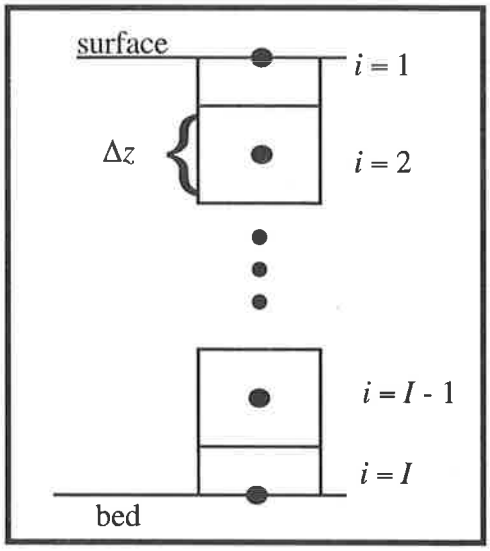

The mass in the water column at time level n is given by:

$$M^n = \Sigma' m_i^n + \frac{1}{2}m_1^n + \frac{1}{2}m_I^n \qquad \text{(A5.6)}$$

where Σ' signifies summation over internal nodes, $i = 2, ..., I–1$. Therefore, using the properties of the control-volume scheme, as in eq. A5.5:

$$M^n = \Sigma' m_i^{n-1} + (m_2)^*_{\text{roof}} - (m_{I-1})^*_{\text{floor}} + \frac{1}{2}m_1^n + \frac{1}{2}m_I^n \qquad \text{(A5.7)}$$

Now define the following volumes: $V = A\Delta z$, $W = Aw_s\Delta t$, $D^n = AK_z^n\Delta t/\Delta z$, $F = A\alpha\Delta t$. The approximations used for the 2nd and 3rd right-hand-side terms in eq. A5.7 are

$$(m_2)^*_{\text{roof}} = \frac{W}{4}(B_1^n+B_2^n+B_1^{n-1}+B_2^{n-1}) - \frac{1}{2}[D^n(B_2^n-B_1^n) + D^{n-1}(B_2^{n-1}-B_1^{n-1})] \qquad \text{(A5.8)}$$

$$(m_{I-1})^*_{\text{floor}} = \frac{W}{4}(B_{I-1}^n+B_I^n+B_{I-1}^{n-1}+B_I^{n-1}) - \frac{1}{2}[D^n(B_I^n-B_{I-1}^n) + D^{n-1}(B_I^{n-1}-B_{I-1}^{n-1})] \qquad \text{(A5.9)}$$

To approximate the last two terms in eq. A5.7 it is appropriate to use

$$\frac{1}{2}m_1^n = \frac{V}{2}B_1^n \qquad \text{(A5.10)}$$

$$\frac{1}{2}m_I^n = \frac{V}{2}B_I^n \qquad \text{(A5.11)}$$

Therefore the mass balance (eq. A5.7) becomes:

$$M^n = \Sigma' m_i^{n-1} + \frac{1}{4}[(W+2D^n+2V)B_1^n + (W-2D^n)B_2^n + (W+2D^{n-1})B_1^{n-1} + (W-2D^{n-1})B_2^{n-1} - (W+2D^n)B_{I-1}^n - (W-2D^n-2V)B_I^n - (W+2D^{n-1})B_{I-1}^{n-1} - (W-2D^{n-1})B_I^{n-1}] \quad \text{(A5.12)}$$

We want the first right-hand-side term in this equation to be M^{n-1}—any residual terms would quantify the mass balance error. To do this we use the boundary condition formulations used by Cloern to get rid of the terms B_1^n and B_I^n, and collect up the appropriate coefficients.

For the first boundary condition [i.e., $(K_z \partial B/\partial z - w_s B)_{z=0} = 0$] Cloern used:

$$\frac{1}{2}[D^n(B_2^n - B_1^n) + D^{n-1}(B_2^{n-1} - B_1^{n-1})] - \frac{W}{2}(B_1^n + B_1^{n-1}) = 0 \quad \text{(A5.13)}$$

from which

$$B_1^n = [D^n B_2^n - (W+D^{n-1})B_1^{n-1} + D^{n-1}B_2^{n-1}]/(W+D^n) \quad \text{(A5.14)}$$

For the bottom boundary condition [i.e., $(K_z \partial B/\partial z - w_s B)_{z=H} = -\alpha B_{z=H}$] Cloern used

$$\frac{1}{2}[D^n(B_I^n - B_{I-1}^n) + D^{n-1}(B_I^{n-1} - B_{I-1}^{n-1})] - \frac{W}{2}(B_{I-1}^n + B_{I-1}^{n-1}) = -\frac{F}{2}(B_I^n + B_I^{n-1}) \quad \text{(A5.15)}$$

Note that the advective term (3rd group of terms on the left-hand-side) was approximated at node $I-1$, not at the boundary node (I), presumably because $w_s = 0$ at the boundary. (This kind of arbitrariness is avoided in a control-volume approach.)

From eq. A5.15

$$B_I^n = [(W+D^n)B_{I-1}^n + (W+D^{n-1})B_{I-1}^{n-1} - (F+D^{n-1})B_I^{n-1}]/(F+D^n) \quad \text{(A5.16)}$$

We can obtain the desired result by: (i) substituting eqs. A5.14 & A5.16 into eq. A5.12, (ii) noting from eqs. A5.6, A5.10 & A5.11 that $M^{n-1} = \Sigma' m_i^{n-1} + \frac{V}{2}B_1^{n-1} + \frac{V}{2}B_I^{n-1}$, and (iii) setting $F = 0$ (because we set $\alpha = 0$). The result is:

$$M^n = M^{n-1} + \left(\frac{2VD^n+W^2}{4(W+D^n)}\right)B_2^n - \left(V+\frac{\Delta D(W-2V)}{4(W+D^n)}\right)B_1^{n-1} +$$
$$\left(\frac{2VD^{n-1}+W(W+\Delta D)}{4(W+D^n)}\right)B_2^{n-1} + \left(\frac{2V(W+D^n)-W^2}{4D^n}\right)B_{I-1}^n -$$
$$\left(V+\frac{\Delta D(W-2V)}{4D^n}\right)B_I^{n-1} + \left(\frac{2V(W+D^{n-1})-W(W-\Delta D)}{4D^n}\right)B_{I-1}^{n-1} \qquad \text{(A5.17)}$$

where $\Delta D = D^n - D^{n-1}$. The final six terms thus comprise a mass balance error. Note that for pure diffusion ($W = 0$) and constant diffusivity ($D^n = D^{n-1}$, so $\Delta D = 0$) we get

$$M^n = M^{n-1} + \frac{V}{2}\left[(B_2^n - 2B_1^{n-1} + B_2^{n-1}) + (B_{I-1}^n - 2B_I^{n-1} + B_{I-1}^{n-1})\right] \qquad \text{(A5.18)}$$

For a uniform initial condition the bracketed term = 0 algebraically. However numerical tests show that this difference equation magnifies rounding errors, so that mass is falsified even for pure diffusion.

NIWA Ecosystems
National Institute of Water and Atmospheric Research
P. O. Box 11–115, Hamilton, New Zealand